

NLO QCD corrections to inclusive $b \rightarrow c\ell\bar{\nu}$ decay spectra up to $1/m_Q^3$

Thomas Mannel, Daniel Moreno[✉], and Alexei A. Pivovarov[✉]

Center for Particle Physics Siegen, Theoretische Physik 1, Universität Siegen, 57068 Siegen, Germany



(Received 16 December 2021; accepted 7 March 2022; published 30 March 2022)

We present analytical results for higher order corrections to the decay spectra of inclusive semileptonic heavy hadron weak decays, using the heavy quark expansion (HQE). We compute analytically the spectrum of the leptonic invariant mass for $B \rightarrow X_c \ell\bar{\nu}$ up to and including terms of order $1/m_Q^3$ within the HQE at next-to-leading order in α_s . The full dependence of the differential rate on the mass of the final-state quark is taken into account. We discuss the implications of our results for the precision determination of the Cabibbo-Kobayashi-Maskawa matrix element $|V_{cb}|$.

DOI: 10.1103/PhysRevD.105.054033

I. INTRODUCTION

Testing the flavor sector of the Standard Model (SM) is one of the major current activities in particle physics. On the experimental side large experimental activities are under way, which started with the construction of B factories about two decades ago, and efforts are continuing with the Belle II experiment at the Kō-Enerugī butsurigaku Kenkyūsho (KEK) Super Flavor Factory in Tsukuba (Japan) and at the LHCb experiment at the Large Hadron Collider (LHC) at CERN in Geneva (Switzerland).

From the theoretical side, enormous progress has been made over the last three decades. Making use of the fact that the b -quark mass (and to some extent also the c -quark mass) are largely compared to the QCD scale Λ_{QCD} , precision methods have been developed, which allow us to perform a combined expansion in Λ_{QCD}/m_Q and $\alpha_s(m_Q)$ [1–4], resulting in precision predictions with controllable uncertainties.

All this has established the flavor structure of the SM, namely the Cabibbo-Kobayashi-Maskawa (CKM) picture of quark mixing at the precision level, leaving only limited room for physics beyond the SM (BSM). However, some recent data show persistent tensions with the SM predictions, the so-called B anomalies, which could be interpreted as first signals for BSM effects. To this end, precision quark-flavor physics may become an important tool to establish the presence of BSM effects. However, this requires—aside from more precise measurements—very precise theoretical calculations, which require in the field of flavor physics also to deal with nonperturbative effects. In

the context of the heavy quark expansion (HQE) this means to push for higher orders in both Λ_{QCD}/m_Q and $\alpha_s(m_Q)$.

One important example is the calculation of the differential rate for the inclusive $B \rightarrow X_c \ell\bar{\nu}$ within the HQE[5–8], which is the key ingredient for the precision determination of $|V_{cb}|$ from inclusive decays, where a theoretical uncertainty of less than two percent has been achieved. In fact, the tension between the values of $|V_{cb}|$ ($x = u, c$) extracted from inclusive and exclusive decays is one of the persistent B anomalies.

The HQE hadronic parameters constitute the nonperturbative input into the HQE. The number of independent parameters strongly proliferates at higher orders, thereby limiting our possibilities for a fully model independent determination of $|V_{cb}|$ from inclusive decays. Up to $(\Lambda_{\text{QCD}}/m_Q)^3$ only four HQE parameters emerge, which can be extracted from the measurement of moments of the charged lepton energy spectrum and the hadronic invariant mass spectrum, but starting at $(\Lambda_{\text{QCD}}/m_Q)^4$ the number of independent HQE parameters is too large to be extracted from data.

However, it has been shown in [9,10] that one may exploit a symmetry of the HQE, the so-called reparametrization invariance (RPI), which allows one to reduce the number of independent HQE parameters for specific observables. For the case at hand, the inclusive semileptonic $B \rightarrow X_c \ell\bar{\nu}$ decays, these observables are all related to the spectrum of the leptonic invariant mass. Based on this approach a further improvement of the precision of the inclusive $|V_{cb}|$ determination is expected since the reduced number of HQE parameters can be determined from the data.

The current status of the HQE calculation of $B \rightarrow X_c \ell\bar{\nu}$ is already quite elaborate. The leading term, i.e., the partonic rate is known at next-to-next-to-leading order ($N^2\text{LO}$)-QCD [11–24] and at next-to-next-to-next-to-leading order ($N^3\text{LO}$) only for the total rate [25]. The first

Published by the American Physical Society under the terms of the [Creative Commons Attribution 4.0 International license](#). Further distribution of this work must maintain attribution to the author(s) and the published article's title, journal citation, and DOI. Funded by SCOAP³.

power correction, of order $(\Lambda_{\text{QCD}}/m_Q)^2$, is known as next-to-leading order (NLO)-QCD [6–8,26–31]. The second power correction, of order $(\Lambda_{\text{QCD}}/m_Q)^3$, is known at LO-QCD [32,33] and at NLO-QCD only for the total width [34]. Finally, third and fourth power corrections, of order $(\Lambda_{\text{QCD}}/m_Q)^{4,5}$ have been computed at LO-QCD in [35,36].

In the present paper we give an analytical result for the leptonic invariant mass spectrum at order $\alpha_s(m_Q)(\Lambda_{\text{QCD}}/m_Q)^3$. We also give the analytical result for the $\alpha_s(m_Q)(\Lambda_{\text{QCD}}/m_Q)^2$ terms of the leptonic invariant mass spectrum, which are known up to now only numerically [28]. These results will allow us to extract $|V_{cb}|$ from the RPI method on the basis of analytical expressions.

See Supplemental Material [37] which contains analytical results in *Mathematica* format for the coefficients of the leptonic invariant mass spectrum up to $\mathcal{O}(\alpha_s(m_Q)/m_Q^3)$ and the $\mathcal{O}(\alpha_s(m_Q))$ Darwin coefficients of the moments with a low cut in the leptonic invariant mass.

The paper is organized as follows. In Secs. II and III we set the notation and briefly describe our method for the computation of the differential width. In Secs. IV and V we compute the $(\Lambda_{\text{QCD}}/m_Q)^2$ and $(\Lambda_{\text{QCD}}/m_Q)^3$ HQE coefficients of the leptonic invariant mass spectrum at $\mathcal{O}(\alpha_s(m_Q))$. Finally, we discuss the impact of our results after a brief numerical analysis in Sec. VI. Analytical results for the coefficients are displayed in the Appendix.

II. HQE FOR INCLUSIVE HEAVY FLAVOR DECAYS

We start giving some basics of the theoretical description of inclusive semileptonic decays within the HQE. More details can be found in the literature (e.g., [38]). The effective Fermi Lagrangian \mathcal{L}_{eff} for the semileptonic $b \rightarrow c\ell\bar{\nu}_\ell$ transitions reads

$$\mathcal{L}_{\text{eff}} = 2\sqrt{2}G_F V_{cb}(\bar{b}_L \gamma_\mu c_L)(\bar{\nu}_L \gamma^\mu \ell_L) + \text{H.c.}, \quad (1)$$

with the subscript L denoting the left-handed fermion fields. Here G_F is the Fermi constant, and V_{cb} is the relevant CKM matrix element.

Using the optical theorem, one obtains the inclusive decay rate $B \rightarrow X_c \ell \bar{\nu}_\ell$ from taking an absorptive part of the forward matrix element of the leading order transition operator \mathcal{T} ,

$$\begin{aligned} \mathcal{T} &= i \int dx T\{\mathcal{L}_{\text{eff}}(x)\mathcal{L}_{\text{eff}}(0)\}, \\ \Gamma(B \rightarrow X_c \ell \bar{\nu}_\ell) &\sim \text{Im}\langle B|\mathcal{T}|B\rangle. \end{aligned} \quad (2)$$

Since the heavy quark mass m_b is a large scale compared to the hadronization scale Λ_{QCD} of QCD ($m_Q \gg \Lambda_{\text{QCD}}$), the forward matrix element contains perturbatively calculable contributions. These can be separated from the nonperturbative pieces using the method of effective field theory.

For a heavy hadron with momentum p_B and mass M_B , a large part of the heavy-quark momentum p_b is due to a pure kinematical contribution due to its large mass $p_b = m_b v + \Delta$ with $v = p_B/M_B$ being the velocity of the heavy hadron. The momentum $\Delta \sim \mathcal{O}(\Lambda_{\text{QCD}})$ describes the soft-scale fluctuations of the heavy quark field near its mass shell. This decomposition of the quark momentum is implemented by redefining the heavy quark field $b(x)$,

$$b(x) = e^{-im_b(vx)} b_v(x), \quad (3)$$

so that $\partial b_v(x) \sim \Delta$. Inserting this into (2), we get

$$\mathcal{T} = i \int dx e^{im_b v \cdot x} T\{\tilde{\mathcal{L}}_{\text{eff}}(x)\tilde{\mathcal{L}}_{\text{eff}}(0)\}, \quad (4)$$

where $\tilde{\mathcal{L}}$ is the same expression as \mathcal{L} with the replacement $b(x) \rightarrow b_v(x)$.

This expression allows one to set up the HQE as an expansion in Λ_{QCD}/m_b by matching the imaginary part of the transition operator \mathcal{T} in QCD to an expansion in inverse powers of the heavy quark mass using local operators defined in heavy quark effective theory (HQET) [39,40] with matching coefficients C_i ,

$$\begin{aligned} \text{Im}\mathcal{T} &= \Gamma^0 |V_{cb}|^2 \left(C_0 \mathcal{O}_0 + C_v \frac{\mathcal{O}_v}{m_b} + C_\pi \frac{\mathcal{O}_\pi}{2m_b^2} + C_G \frac{\mathcal{O}_G}{2m_b^2} \right. \\ &\quad \left. + C_D \frac{\mathcal{O}_D}{4m_b^3} + C_{LS} \frac{\mathcal{O}_{LS}}{4m_b^3} \right). \end{aligned} \quad (5)$$

The HQET operators \mathcal{O}_i are listed below ordered by their mass dimension up to dimension six:

$$\mathcal{O}_0 = \bar{h}_v h_v \quad (\text{mass dimension three}), \quad (6)$$

$$\mathcal{O}_v = \bar{h}_v v \cdot \pi h_v \quad (\text{mass dimension four}), \quad (7)$$

$$\mathcal{O}_\pi = \bar{h}_v \pi_\perp^2 h_v \quad (\text{mass dimension five}), \quad (8)$$

$$\mathcal{O}_G = \frac{1}{2} \bar{h}_v [\gamma^\mu, \gamma^\nu] \pi_{\perp\mu} \pi_{\perp\nu} h_v \quad (\text{mass dimension five}), \quad (9)$$

$$\mathcal{O}_D = \bar{h}_v [\pi_{\perp\mu}, [\pi_\perp^\mu, v \cdot \pi]] h_v \quad (\text{mass dimension six}), \quad (10)$$

$$\mathcal{O}_{LS} = \frac{1}{2} \bar{h}_v [\gamma^\mu, \gamma^\nu] \{\pi_{\perp\mu}, [\pi_{\perp\nu}, v \cdot \pi]\} h_v \quad (\text{mass dimension six}), \quad (11)$$

where $\pi_\mu = iD_\mu = i\partial_\mu + g_s A_\mu^a T^a$ is the covariant derivative of QCD, $\pi^\mu = v^\mu(v\pi) + \pi_\perp^\mu$ and where we have neglected operators which are of higher dimension on shell. Here the field h_v is the HQET field, whose dynamics are determined by the HQET Lagrangian [40].

It is convenient to choose the local operator $\bar{b} \not{=} b$ defined in full QCD as the leading term of the HQE in Eq. (5)

instead of \mathcal{O}_0 since its forward matrix element with hadronic states is absolutely normalized. The HQE of the operator $\bar{b}\not{p}b$ reads

$$\begin{aligned}\bar{b}\not{p}b &= \mathcal{O}_0 + \tilde{C}_v \frac{\mathcal{O}_v}{m_b} + \tilde{C}_\pi \frac{\mathcal{O}_\pi}{2m_b^2} + \tilde{C}_G \frac{\mathcal{O}_G}{2m_b^2} \\ &\quad + \tilde{C}_D \frac{\mathcal{O}_D}{4m_b^3} + \tilde{C}_{LS} \frac{\mathcal{O}_{LS}}{4m_b^3},\end{aligned}\quad (12)$$

with the matching coefficients \tilde{C}_i being pure numbers. Eventually, we use the equations of motion (EOM) of the HQET Lagrangian to get rid of the operator \mathcal{O}_v in Eq. (5).

Thus, the HQE for semileptonic weak decays is written as (e.g., [41])

$$\Gamma(B \rightarrow X_c \ell \bar{\nu}_\ell) = \Gamma^0 |V_{cb}|^2 \left[C_0 - C_{\mu_\pi} \frac{\mu_\pi^2}{2m_b^2} + C_{\mu_G} \frac{\mu_G^2}{2m_b^2} \right. \\ \left. - C_{\rho_D} \frac{\rho_D^3}{2m_b^3} - C_{\rho_{LS}} \frac{\rho_{LS}^3}{2m_b^3} \right], \quad (13)$$

where $\Gamma^0 = G_F^2 m_b^5 / (192\pi^3)$, and m_b is the b -quark mass. The coefficients C_i , $i = 0, \mu_\pi, \mu_G, \rho_D, \rho_{LS}$ depend (in case of neglecting the lepton and light-quark masses) on the ratio $\rho = m_c^2/m_b^2$, where m_c is the c -quark mass. Note that from reparametrization invariance $C_0 = C_{\mu_\pi}$ and $C_{\mu_G} = C_{\rho_{LS}}$ [9,42].

The parameters μ_π^2 , μ_G^2 , ρ_D^3 , and ρ_{LS}^3 are forward matrix elements of local operators usually called the hadronic parameters of the HQE. The definition of these parameters in our calculation reads

$$\langle B(p_B) | \bar{b}\not{p}b | B(p_B) \rangle = 2M_B, \quad (14)$$

$$-\langle B(p_B) | \mathcal{O}_\pi | B(p_B) \rangle = 2M_B \mu_\pi^2, \quad (15)$$

$$c_F(\mu) \langle B(p_B) | \mathcal{O}_G | B(p_B) \rangle = 2M_B \mu_G^2, \quad (16)$$

$$-c_D(\mu) \langle B(p_B) | \mathcal{O}_D | B(p_B) \rangle = 4M_B \rho_D^3, \quad (17)$$

$$-c_S(\mu) \langle B(p_B) | \mathcal{O}_{LS} | B(p_B) \rangle = 4M_B \rho_{LS}^3, \quad (18)$$

where the forward matrix elements are taken over the physical state of the heavy meson or, theoretically, in full QCD [9]. The quantities $c_F(\mu)$, $c_D(\mu)$, and $c_S(\mu)$ are matching coefficients in the HQET Lagrangian with μ being the renormalization point. The NLO expressions for these coefficients are known. The expression given in Eq. (13) emerges from the direct matching of the QCD expression for the transition operator to HQET. Taking the forward matrix element of Eq. (5) after using the HQE of the $\bar{b}\not{p}b$ operator and the EOM of the HQET Lagrangian yields Eq. (13).

In general, there is an additional operator $\mathcal{O}_I = \bar{h}_v(v\pi)^2 h_v$ in the complete basis of dimension five

operators, however, it will be of higher order in the HQE after using the EOM of HQET. Similarly, there are five additional operators at dimension six, which vanish (or become of higher order in the power expansion) after using the EOM.

The coefficients C_i have a perturbative expansion in the strong coupling constant $\alpha_s(m_b)$. The leading coefficient C_0 is known analytically to $\mathcal{O}(\alpha_s^2)$ precision in the massless limit for the final state quark [43]. At this order, the mass corrections have been analytically accounted for the total width as an expansion in the mass of the final fermion in [20] and for the differential distribution in [19]. For the total rate, $\mathcal{O}(\alpha_s^3)$ corrections have been computed quite recently [25] with mass corrections of the final state quark, again accounted as an expansion.

The coefficient of the kinetic energy parameter is linked to the coefficient C_0 by reparametrization invariance (for an explicit check see, e.g., [26]). The NLO correction to the coefficient of the chromomagnetic parameter $C_{\mu_G^2}$ has been investigated in [28], where the hadronic tensor has been computed analytically, and the total decay rate has been then obtained by direct numerical integration over the phase space. This calculation allows for the application of different energy/momenta cuts in the phase space necessary for the accurate comparison with experimental data.

III. LEPTON INVARIANT MASS SPECTRUM: GENERALITIES

In this section we will discuss the setup for the calculation of the differential rate in the leptonic invariant mass squared, $r = q^2/m_b^2$. While the relevant scale of the process in the experimental setup is represented by the physical B -meson mass, in theory the parameter that enters the calculation is the b -quark mass. Therefore, it is the quark mass that sets the scale of the theoretical computation in QCD and defines the dimensionless parameter r . We follow the general procedure described in [44] and use the dispersion representation of the one-loop diagram to write the lepton-neutrino loop as an integral differential in the lepton pair invariant mass squared. In this way the leptonic loop becomes an “effective massive propagator” of mass q .

We assume the leptons to be massless, which leads to

$$\begin{aligned}\int \frac{d^D k}{(2\pi)^D} \frac{-\text{Tr}(\Gamma^\sigma i(\not{k} + \not{q}_2)\Gamma^\rho i\not{k})}{k^2(k+q_2)^2} \\ = i \int_0^\infty d(q^2) \frac{\rho_s(q^2)}{q^2 - q_2^2 - i\eta} (q_2^2 g^{\rho\sigma} - q_2^\rho q_2^\sigma), \\ \Gamma_\mu = \gamma_\mu \frac{1}{2} (1 - \gamma_5),\end{aligned}\quad (19)$$

where $D = 4 - 2\epsilon$, q_2 is the four-momentum flowing through the leptons, and the spectral density ρ_s to $\mathcal{O}(\epsilon^0)$ is a constant

$$\rho_s(q^2) = \frac{2}{3} \frac{1}{16\pi^2} + \mathcal{O}(\epsilon). \quad (20)$$

Since renormalization can be performed at the differential level, the integrand is finite, and it is enough to keep the $\mathcal{O}(\epsilon^0)$ term in ρ_s .

The purely leptonic part is not affected by QCD corrections, which keeps the spectral density very simple. Note that the effective massive propagator of mass q is transverse due to the fact that the leptons are massless. After writing the leptonic loop in this form, we can compute the width differential in the dilepton pair invariant mass squared, which we write as it follows:

$$\begin{aligned} & \frac{d\Gamma(B \rightarrow X_c \ell \bar{\nu}_\ell)}{dr} \\ &= \Gamma^0 |V_{cb}|^2 \rho_s \left[C_0 - C_{\mu_\pi} \frac{\mu_\pi^2}{2m_b^2} + C_{\mu_G} \frac{\mu_G^2}{2m_b^2} - C_{\rho_D} \frac{\rho_D^3}{2m_b^3} - C_{\rho_{LS}} \frac{\rho_{LS}^3}{2m_b^3} \right] \\ &= \Gamma^0 |V_{cb}|^2 \rho_s \left[C_0 \left(1 - \frac{\bar{C}_\pi - \bar{C}_v}{C_0} \frac{\mu_\pi^2}{2m_b^2} \right) + \left(\frac{\bar{C}_G}{c_F(\mu)} - \bar{C}_v \right) \frac{\mu_G^2}{2m_b^2} \right. \\ &\quad \left. - \left(\frac{\bar{C}_D}{c_D(\mu)} - \frac{1}{2} \bar{C}_v \right) \frac{\rho_D^3}{2m_b^3} - \left(\frac{\bar{C}_{LS}}{c_S(\mu)} - \frac{1}{2} \bar{C}_v \right) \frac{\rho_{LS}^3}{2m_b^3} \right], \end{aligned} \quad (21)$$

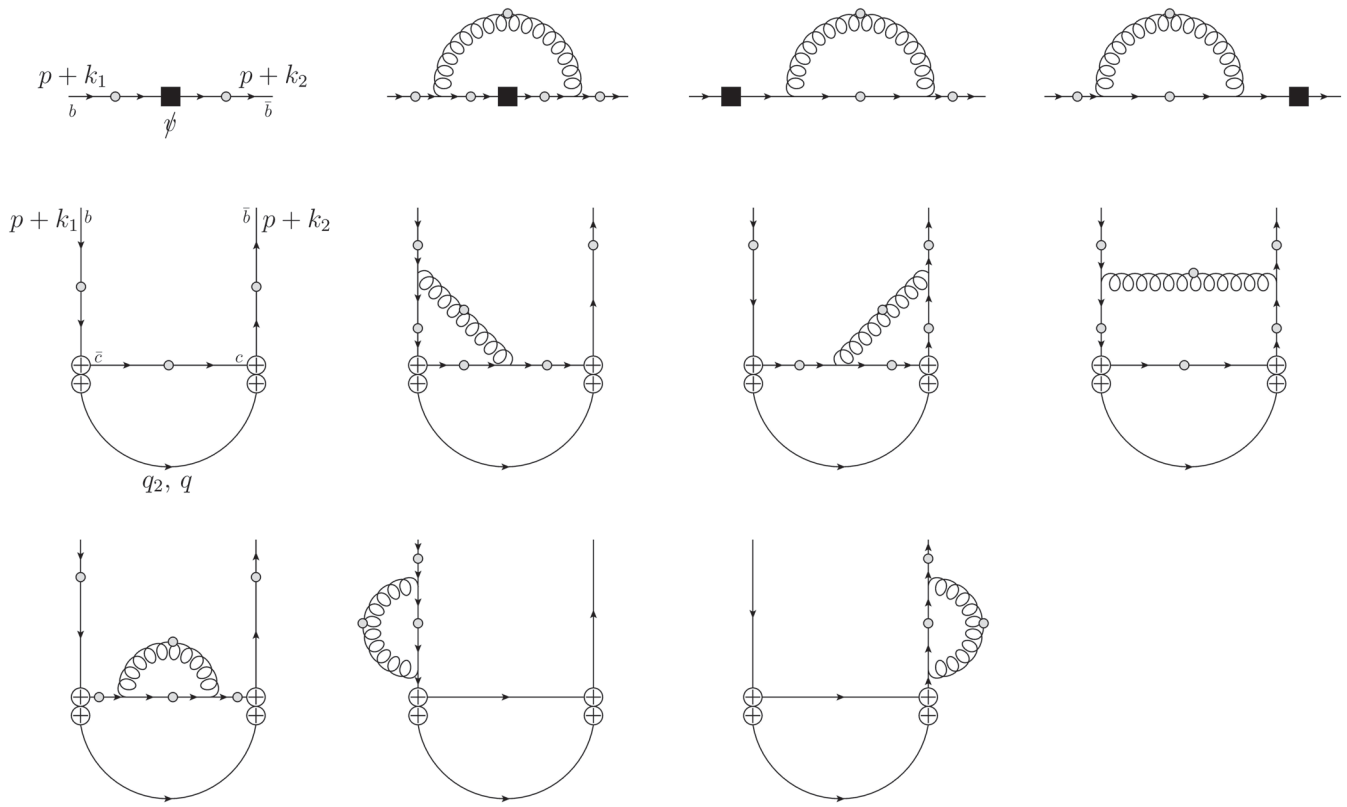


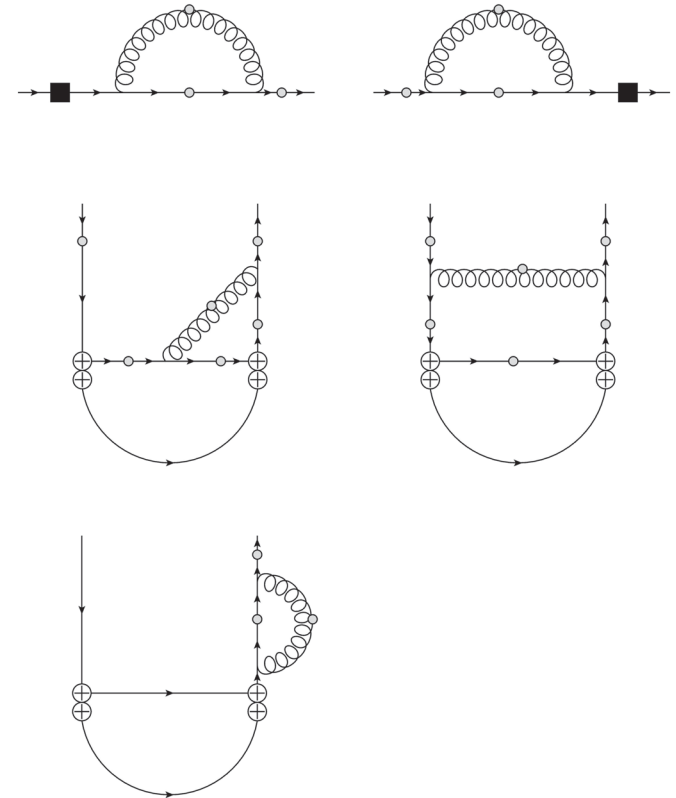
FIG. 1. Quark to quark-gluon scattering diagrams contributing to the coefficients $\bar{C}_i = C_i - C_0 \tilde{C}_i$ of power corrections in the HQE of the $b \rightarrow c \ell \bar{\nu}_\ell$ decay spectrum, Eq. (21). Black squares stand for \not{p} insertions, circles with crosses for insertions of the operator in \mathcal{L}_{eff} , and grey dots stand for possible gluon insertions with incoming momentum $k_2 - k_1$. After properly accounting for all one gluon insertions, there are five diagrams at LO-QCD and 41 diagrams at NLO-QCD.

where $0 \leq r \leq (1 - \sqrt{\rho})^2$, and we have defined $\bar{C}_i \equiv C_i - C_0 \tilde{C}_i$ as the difference between the coefficients C_i of the HQE of the transition operator (in differential form) and the current multiplied by C_0 . The coefficients C_i of the differential rate depend on two variables r and ρ and are related to the coefficients of the total rate by

$$C_i(\rho) = \int_0^{(1-\sqrt{\rho})^2} dr \rho_s \mathcal{C}_i(r, \rho). \quad (22)$$

As discussed in Ref. [10] one can reduce the number of independent HQE parameters by using reparametrization-invariant observables, and the lepton invariant mass spectrum is such a quantity. However, in the same way as for the lepton energy moments, the resulting expression cannot be interpreted point-by-point, and so one refers to moments of the spectra, for which a clean HQE exists. In addition, it may be necessary from the experimental side to introduce cuts on the variables, for which the leptonic invariant mass still preserves RPI.

Consequently, we discuss the (not yet normalized) moments with a lower cut r_{\min} and upper cut r_{\max} that are defined as



$$M_n(\rho, r_{\min}, r_{\max}) = \int_{r_{\min}}^{r_{\max}} dr r^n \frac{d\Gamma(r, \rho)}{dr}, \quad (23)$$

with $0 < r_{\min} < r_{\max} < (1 - \sqrt{\rho})^2$. Since we derive analytical expressions for the leptonic invariant mass spectrum, the above quantity can be readily evaluated numerically, except for the Darwin coefficient, which requires keeping $D = 4 - 2\epsilon$ in order to regularize the IR divergence that appears at the end of the integration region for r .

For the leading power, the Feynman diagrams contributing to the differential width at LO-QCD and NLO-QCD are one-loop and two-loop quark to quark scattering diagrams. For the computation of power corrections, the LO-QCD and NLO-QCD contributions are represented by one-loop and two-loop quark to quark-gluon scattering Feynman diagrams, respectively. The latter are shown in Fig. 1.

By using LiteRed [45,46] the corresponding amplitude is reduced to a combination of the master integrals computed in Ref. [44]. We use standard dimensional regularization in $D = 4 - 2\epsilon$ spacetime dimensions. Algebraic manipulations, including Dirac algebra, are carried out with the help of Tracer [47]. Expansion of hypergeometric functions is done with the help of HypExp [48,49]. The computation is done in the Feynman gauge, and we use the background field method to compute the scattering in the external gluonic field.

We adopt the $\overline{\text{MS}}$ renormalization scheme (e.g., [50]) for the renormalization of the strong coupling $\alpha_s(\mu)$ and the HQET Lagrangian. The bottom and charm quarks will be renormalized on shell. In practice, that is $b_B = (Z_2^{\text{OS}})^{1/2} b$ and $m_{c,B} = Z_{m_c}^{\text{OS}} m_c$, where the subscript B denotes bare quantities, the ones with no subscript stand for renormalized, and

$$Z_{m_q}^{\text{OS}} = 1 - C_F \frac{\alpha_s(\mu)}{4\pi} \left(\frac{3}{\epsilon} + 6 \ln \left(\frac{\mu}{m_q} \right) + 4 \right), \quad (24)$$

with $Z_2^{\text{OS}} = Z_{m_b}^{\text{OS}}$ to this order. Also $g_{s,B}^2 = 4\pi Z_g^2 \alpha_s(\mu) \bar{\mu}^{2\epsilon}$, where $\bar{\mu}^2 = \mu^2 (e^{\gamma_E}/4\pi)$, is the $\overline{\text{MS}}$ renormalization scale. For the precision of the calculation, the renormalization factor of the strong coupling is only needed at tree level ($Z_g = 1$). The $SU(3)$ color factors are $C_F = 4/3$ and $C_A = 3$.

We quote our results in the on-shell scheme for both quark masses m_c and m_b . For more precise predictions one usually chooses for the bottom quark a low-scale short distance mass, such as the kinetic or the $1S$ mass, and thus one needs to convert the on-shell mass into such a mass scheme. However, the known one-loop expression will be sufficient. For the charm quark mass, we are free to choose still a different renormalization scheme; one can either renormalize it on shell or in the $\overline{\text{MS}}$ scheme. We have chosen the former because results become slightly more

compact in that scheme, and thus quote our results in the on-shell scheme. A change in the scheme can easily be achieved by using the relation between the $\overline{\text{MS}}$ and pole masses at one-loop order,

$$m_c^{\text{pole}} = m_c^{\overline{\text{MS}}}(\mu) \left(1 + C_F \frac{\alpha_s}{4\pi} \left(6 \ln \left(\frac{\mu}{m_c} \right) + 4 \right) \right). \quad (25)$$

IV. DIFFERENTIAL RATE IN THE LEPTON INVARIANT MASS AT $\mathcal{O}(1/m_b^2)$

The NLO correction to the terms at order $1/m_b^2$ have been computed already a while ago [26–31], but to the best of our knowledge there is no analytical expression for the leptonic invariant-mass spectrum in the literature. The coefficient of μ_π^2 can be inferred from the leading order term in the HQE, whereas the coefficient of μ_G^2 must be computed explicitly. For the computation of the chromomagnetic term, we follow the approach used earlier for the calculation of the total width [29–31].

One takes the amplitude of quark to quark-gluon scattering, expands to linear order in the small momentum, and projects it to the corresponding dimension five HQET operator. At dimension five the operators (8) and (9) appear together with the operator $\mathcal{O}_1 = \bar{h}_v(v \cdot \pi)^2 h_v$, which is irrelevant because it is of higher order due to the EOM.

The contribution to the chromomagnetic coefficient is obtained by considering a single small gluon momentum k_\perp and picking up the contribution antisymmetric in $k_\perp \epsilon_\perp$, where ϵ is the gluon polarization vector. Incoming and outgoing bottom quarks carry momentum p and $p + k_\perp$, respectively, with $p^2 = m_b^2$.

First, we directly compute the difference between the HQE of the transition operator and the current

$$\bar{\mathcal{C}}_G \equiv \mathcal{C}_G - \mathcal{C}_0 \tilde{\mathcal{C}}_G = Z_2^{\text{ON}} Z_{\mathcal{O}_G} (\mathcal{C}_G^{\text{bare}} - \mathcal{C}_0^{\text{bare}} \tilde{\mathcal{C}}_G^{\text{bare}}), \quad (26)$$

where

$$Z_{\mathcal{O}_G} = 1 - C_A \frac{\alpha_s}{4\pi \epsilon} \quad (27)$$

is the renormalization constant of the chromomagnetic operator. The quantity $\bar{\mathcal{C}}_G$ is finite. Once determined, the coefficient in front of the matrix element in the differential width \mathcal{C}_{μ_G} is given by

$$\mathcal{C}_{\mu_G} = \frac{\bar{\mathcal{C}}_G}{c_F(\mu)} - \bar{\mathcal{C}}_v, \quad (28)$$

where

$$c_F(\mu) = 1 + \frac{\alpha_s}{2\pi} \left[C_F + C_A \left(1 + \ln \left(\frac{\mu}{m_b} \right) \right) \right] \quad (29)$$

is the coefficient of the chromomagnetic operator in the HQET Lagrangian [40].

We still have to discuss how to compute the coefficient \bar{C}_v . In order to obtain it one takes the amplitude of quark to quark-gluon scattering, expands to zeroth order in the small momentum, and projects it to the corresponding HQET operator. The contribution to the \mathcal{O}_v coefficient is obtained by considering a longitudinally polarized gluon exchange ($v \cdot \epsilon$) without momentum transfer. Incoming and outgoing bottom quarks carry momentum p , with $p^2 = m_b^2$. Like in the previous case, we directly compute the difference between the HQE of the transition operator and the current

$$\bar{C}_v \equiv \mathcal{C}_v - \mathcal{C}_0 \tilde{\mathcal{C}}_v = Z_2^{\text{ON}} (\mathcal{C}_v^{\text{bare}} - \mathcal{C}_0^{\text{bare}} \tilde{\mathcal{C}}_v^{\text{bare}}). \quad (30)$$

After integration over r in its whole allowed range, we obtain the known results for the coefficients of the total width C_v and C_{μ_G} obtained in Refs. [29–31]. We take the occasion to correct a misprint in Eq. (84) of Ref. [31]. The last term should carry an overall minus sign instead of a plus sign.

The resulting expressions are somewhat lengthy, and we give the analytical result in Appendix A. See also Supplemental Material [37] for results in *Mathematica* format.

V. DIFFERENTIAL RATE IN THE LEPTON INVARIANT MASS AT $\mathcal{O}(1/m_b^3)$

It has been shown in Ref. [9] that due to RPI only the coefficient of ρ_D^3 needs to be determined at $\mathcal{O}(1/m_b^3)$ since the coefficient of ρ_{LS}^3 can be inferred from the one of μ_G . Thus, we will get the full answer at NLO for reparametrization invariant quantities by computing the coefficient of the Darwin term.

To determine this coefficient one takes the amplitude of quark to quark-gluon scattering, expands to quadratic order in the small momenta, and projects it to the corresponding dimension six HQET operator. At dimension six the operators (10) and (11) appear, together with the following operators:

$$\mathcal{O}_{\text{II}} = \bar{h}_v(v \cdot \pi)\pi_\perp^2 h_v, \quad \mathcal{O}_{\text{III}} = \bar{h}_v\pi_\perp^2(v \cdot \pi)h_v,$$

$$\mathcal{O}_{\text{IV}} = \bar{h}_v(v \cdot \pi)^3 h_v,$$

$$\mathcal{O}_{\text{V}} = \bar{h}_v \frac{1}{2} [\gamma^\mu, \gamma^\nu] \pi_{\perp\mu} \pi_{\perp\nu} (v \cdot \pi) h_v,$$

$$\mathcal{O}_{\text{VI}} = \bar{h}_v(v \cdot \pi) \frac{1}{2} [\gamma^\mu, \gamma^\nu] \pi_{\perp\mu} \pi_{\perp\nu} h_v,$$

which mix with (10) and (11), but they contribute only to higher orders due to the EOM. We disentangle the mixing of such operators with the Darwin term by considering a gluon with longitudinal polarization ($v \cdot \epsilon$), using two quark momenta k_1 and k_2 and picking up the structure $k_{1\perp} k_{2\perp}$ symmetric in k_1, k_2 [34]. The kinematical configuration is such that the incoming and outgoing bottom

quarks carry momentum $p + k_{1\perp}$ and $p + k_{2\perp}$, respectively, with $p^2 = m_b^2$. The gluon carries momentum $k_{2\perp} - k_{1\perp}$. Note that the antisymmetric part gives the spin-orbit term.

The matching is performed by integrating out the charm quark simultaneously with the hard modes of the b quark. This means that we treat m_c^2/m_b^2 as a number of order one in the limit $m_b \rightarrow \infty$, implying that also $m_c \rightarrow \infty$. Therefore, our results cannot be extrapolated to the limit $m_c \rightarrow 0$.

For calculations of radiative corrections, we use dimensional regularization. At NLO the cancellation of poles provides a solid check of the computation. At the $1/m_b^3$ order this cancellation is quite delicate since it requires to consider the mixing between operators of different dimensions, which is known to happen in HQET [51–59].

In analogy to Sec. IV we directly compute the difference between the HQE of the transition operator itself and the current $\bar{b}\not\not b$,

$$\bar{C}_D \equiv \mathcal{C}_D - \mathcal{C}_0 \tilde{\mathcal{C}}_D = Z_2^{\text{ON}} Z_{\mathcal{O}_D} (\mathcal{C}_D^{\text{bare}} - \mathcal{C}_0^{\text{bare}} \tilde{\mathcal{C}}_D^{\text{bare}}) + \delta \bar{C}_D^{\text{mix}}, \quad (31)$$

where

$$Z_{\mathcal{O}_D} = -\frac{1}{6} C_A \frac{\alpha_s}{\pi} \frac{1}{\epsilon}, \quad (32)$$

$$\delta \bar{C}_D^{\text{mix}} = \left[C_F \left(\frac{4}{3} \bar{C}_\pi - \frac{2}{3} \bar{C}_v \right) + C_A \left(\frac{5}{12} \bar{C}_G + \frac{1}{12} \bar{C}_\pi - \frac{1}{4} \bar{C}_v \right) \right] \times \frac{\alpha_s}{\pi} \frac{1}{\epsilon} \quad (33)$$

are the renormalization constant of the Darwin operator and the contribution to the Darwin coefficient coming from the operator mixing in HQET, respectively. The quantity \bar{C}_D is finite.

The corresponding anomalous dimensions in the operator mixing are inferred from the cancellation of poles. Due to the functional structure of the coefficients \mathcal{C}_i , the anomalous dimensions are determined uniquely. After taking into account the combinatorial factors coming from the combined insertion of operators of the HQE and operators of the HQET Lagrangian, we find that the anomalous dimensions proportional to $\bar{C}_D, \bar{C}_G, \bar{C}_\pi$ coincide with known results [52], which is a strong check of the calculation. The presence of the coefficient \bar{C}_v means an admixture to the operator \mathcal{O}_v . Such an admixture was pointed out to be present in [34].

Once \bar{C}_D is determined, the coefficient in front of the matrix element of the differential width \mathcal{C}_{ρ_D} is given by

$$\mathcal{C}_{\rho_D} = \frac{\bar{C}_D}{c_D(\mu)} - \frac{1}{2} \bar{C}_v, \quad (34)$$

where

$$c_D(\mu) = 1 + \frac{\alpha_s}{\pi} \left[C_F \left(-\frac{8}{3} \ln \left(\frac{\mu}{m_b} \right) \right) + C_A \left(\frac{1}{2} - \frac{2}{3} \ln \left(\frac{\mu}{m_b} \right) \right) \right] \quad (35)$$

is the coefficient of the Darwin operator in the HQET Lagrangian [40].

The analytical result for the coefficient $C_{\rho_D}(r, \rho)$ is lengthy. We give it in Appendix A and Supplemental Material [37].

After integration over the lepton invariant mass r in the allowed range, we obtain the coefficient of the total width C_{ρ_D} , which is displayed in Eqs. (C1)–(C3) in the Appendix. Analytical expressions for moments with and without low r cut are also computed and given in Appendix B and C, respectively. Expressions are very lengthy and are provided in the Supplemental Material [37].

For the Darwin term, performing the last integration to obtain the coefficient of the total width or moments is rather subtle since the coefficient is IR singular at the upper integration limit $r = (1 - \sqrt{\rho})^2$, pointing out that expansion in ϵ and integration over r do not commute. The

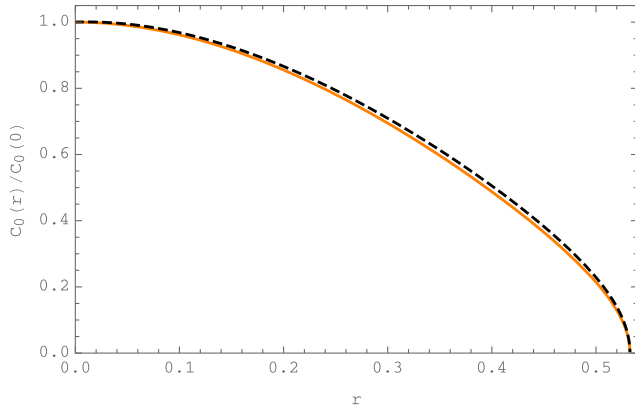
coefficient of the total width and moments can be obtained by restoring the ϵ dependence in the IR singular terms. The IR pole is $(-r + (1 - \sqrt{\rho})^2)^{-3/2-\epsilon}$, whose integral over r is finite in dimensional regularization due to the power $3/2$, and there is no generation of new poles. In other words, the formally divergent integrals are defined in dimensional regularization that may look a bit uneasy if the parameter ϵ is omitted,

$$\int_0^1 \frac{d\zeta}{(1 - \zeta)^{3/2}} = \int_0^1 \frac{d\zeta}{\zeta^{3/2}} = -2 = B\left(-\frac{1}{2}, 1\right) = \frac{\Gamma(-\frac{1}{2})}{\Gamma(\frac{1}{2})}. \quad (36)$$

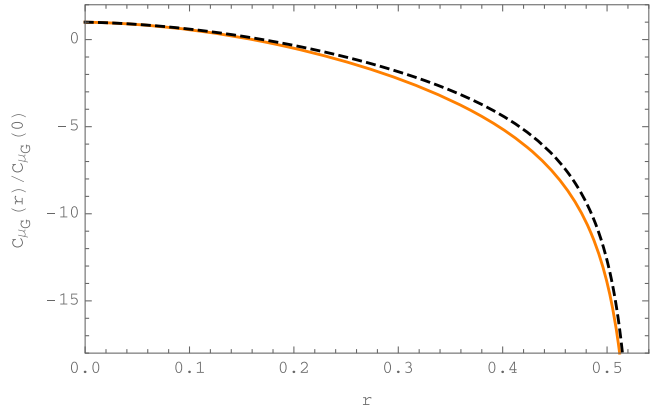
The integral should be understood as a limit at $\epsilon \rightarrow 0$ of the standard dimensionally regularized expression,

$$\int_0^1 \frac{d\zeta}{(1 - \zeta)^{3/2+\epsilon}}. \quad (37)$$

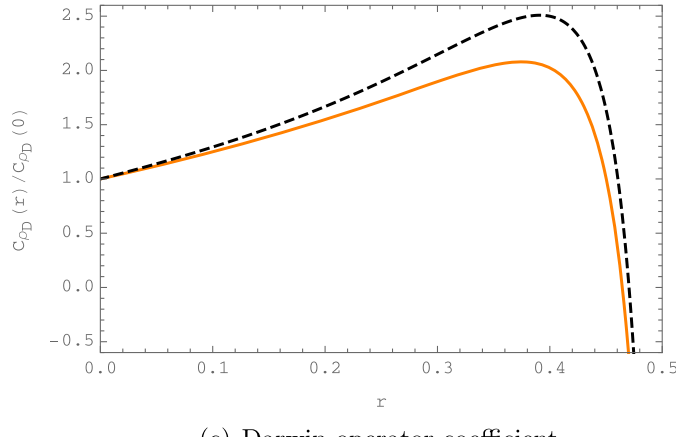
At LO our expression for the total width agrees with the known result [32]. At NLO our result for the total width differs from the first calculation of Ref. [34] based on the



(a) Leading power coefficient.



(b) Chromomagnetic operator coefficient.



(c) Darwin operator coefficient.

FIG. 2. Coefficients of the differential rate normalized to their value at $r = 0$ as a function of the leptonic pair invariant mass squared r . The orange continuous line and the black dashed line stand for coefficients at LO and NLO, respectively.

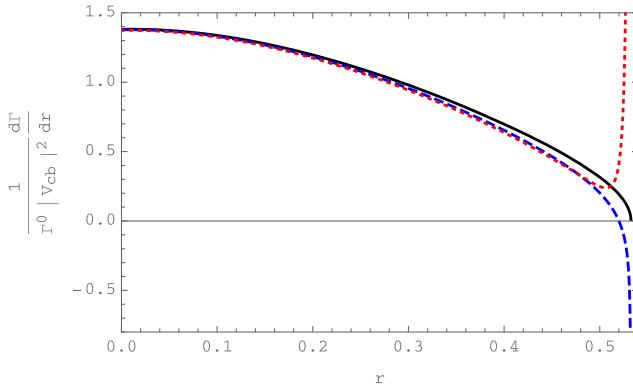
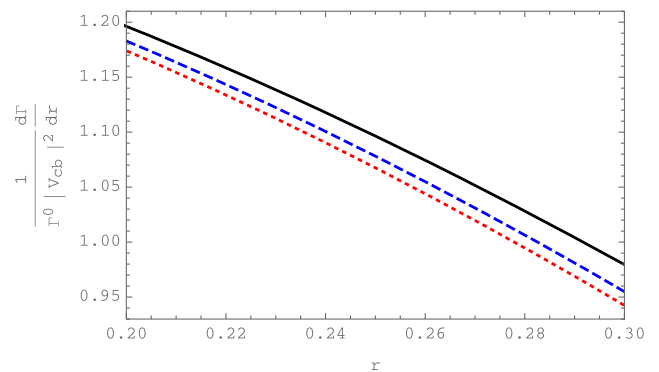
(a) Plot in the allowed range $0 < r < (1 - \sqrt{\rho})^2$.(b) Plot in the range $0.2 < r < 0.3$.

FIG. 3. Differential rate as a function of the lepton pair invariant mass squared r including subsequent power corrections at NLO. The black continuous line stands for the leading power contribution, the blue dashed line includes $1/m_b^2$ corrections, and the red dotted line includes $1/m_b^3$ corrections. The infrared singular behavior at the end of the phase space becomes more abrupt for higher power corrections.

direct use of three-loop Feynman integrals for the total decay rate. Several misprints have been discovered in the code and some terms were overlooked in Ref. [34] that generate the difference with the result of the present paper. However, the general logic of the approach followed in Ref. [34] has proved to be correct as it is confirmed by the actual computation. Therefore, we take Eqs. (C2) and (C3) as our current result for the coefficient of the Darwin term in the HQE of the total width.

To discuss the impact of our result, we show in Figs. 2 and 3 the dependence in the lepton pair invariant mass squared r of the coefficients of the differential rate normalized to their value at $r = 0$ and of the differential rate by including different corrections. We also plot the differential rate in a cut out range in order to perceive the size of corrections. For illustration, we use the typical numerical values displayed in Table I. For the matrix elements these values are taken from [41].

VI. NUMERICAL ANALYSIS

With this paper, the full expression for the leptonic invariant mass spectrum (including also cut moments in the leptonic invariant mass squared) in $b \rightarrow c\ell\bar{\nu}$ decays is

TABLE I. Numerical values of parameters used in plots.

Parameter	Numerical value
$\mu = m_b$	4.8 GeV
$\rho = m_c^2/m_b^2$	0.073
$\alpha_s(m_b)$	0.215
μ_π^2	0.4 GeV ²
μ_G^2	0.35 GeV ²
ρ_D^3	0.2 GeV ³
ρ_{LS}^3	-0.15 GeV ³
$r_{\max} = (1 - \sqrt{\rho})^2$	0.5326
$q_{\max}^2 = m_b^2 r_{\max}$	12.27 GeV ²

known analytically up to the order α_s/m_b^3 with massive final state quark. This will allow one to increase the precision of the $|V_{cb}|$ determination compared to previous analyses by using leptonic invariant mass moments with cuts in this variable. The RPI of HQE is useful for the inclusion of terms of order $1/m_b^4$, where the numerical values of the HQE parameters at this order can be extracted from data [10].

Experimentally, one measures the moments of the spectrum. The low q^2 is difficult to detect and the experimentalist use cuts, while integrating all over the remaining phase space up to the available q^2 . The normalization of the moments onto themselves gives a great deal of simplification experimentally because it requires then only counting events without absolute normalization of the rate. Therefore, the theoretical predictions are written in the form of normalized moments with different cuts,

$$\langle q^{2n} \rangle \equiv m_b^{2n} \hat{M}_n(r_{\text{cut}}) = m_b^{2n} M_n(r_{\text{cut}})/M_0(r_{\text{cut}}). \quad (38)$$

The experimental data set is available with cuts in q^2 from $q_{\text{cut}}^2 = 3.0$ GeV² to $q_{\text{cut}}^2 = 10.0$ GeV² in steps of 0.5 GeV² [60].

We provide the results for the moments in the form

$$M_n(r_{\text{cut}}) = \Gamma^0 |V_{cb}|^2 \left[M_{n,0} \left(1 - \frac{\mu_\pi^2}{2m_b^2} \right) + M_{n,\mu_G} \left(\frac{\mu_G^2}{2m_b^2} - \frac{\rho_{LS}^3}{2m_b^3} \right) - M_{n,\rho_D} \frac{\rho_D^3}{2m_b^3} \right], \quad (39)$$

where

$$\begin{aligned} M_{n,i} &= M_{n,i}^{\text{LO}} + \frac{\alpha_s}{\pi} M_{n,i}^{\text{NLO}} \\ &= M_{n,i}^{\text{LO}} + \frac{\alpha_s}{\pi} (C_F M_{n,i}^{\text{NLO,F}} + C_A M_{n,i}^{\text{NLO,A}}). \end{aligned} \quad (40)$$

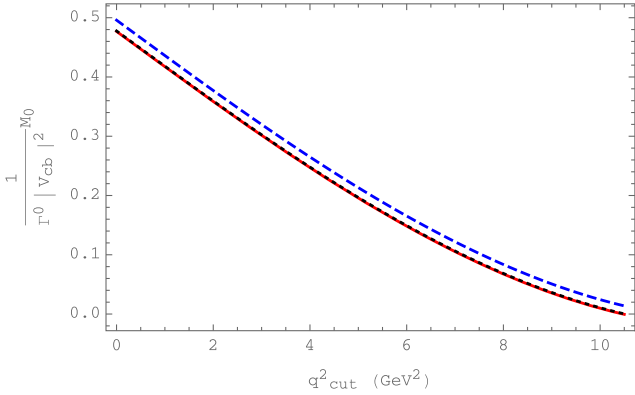
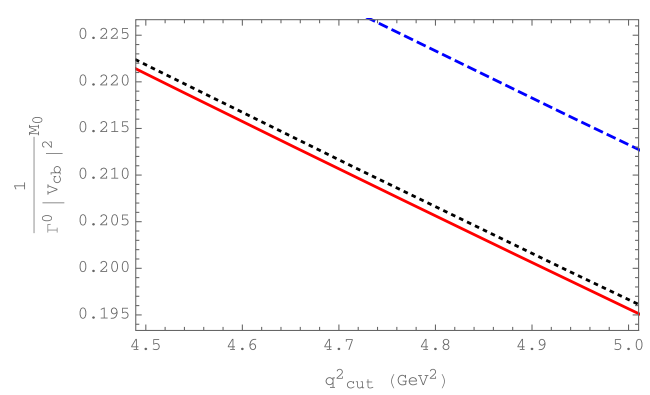
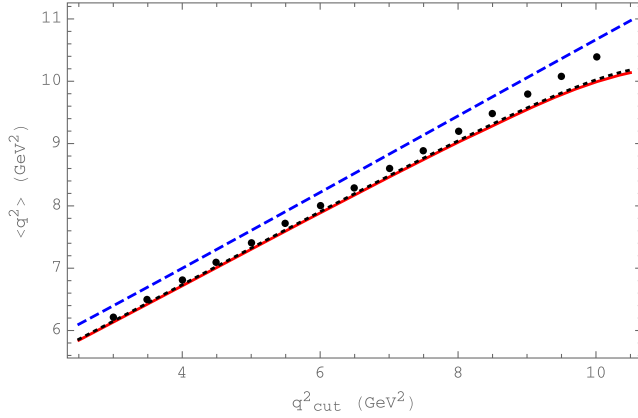
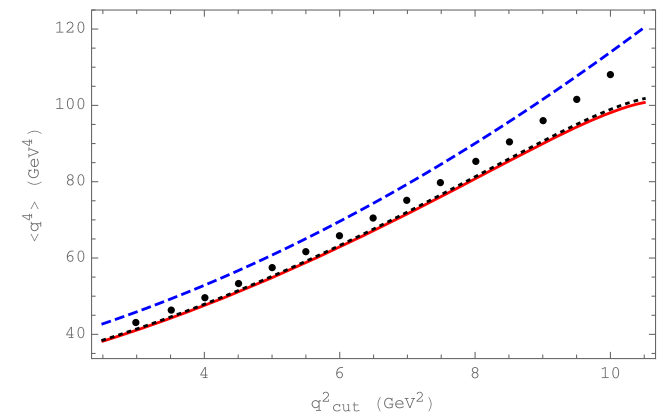
(a) Plot in the range $q_{\text{cut}}^2 < 10.5 \text{ GeV}^2$.(b) Plot in the range $4.5 \text{ GeV}^2 < q_{\text{cut}}^2 < 5 \text{ GeV}^2$.

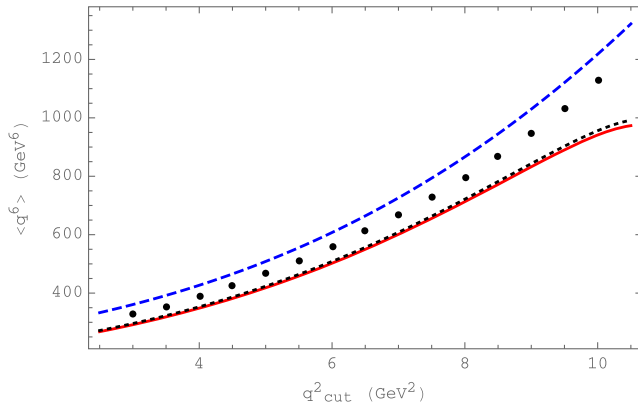
FIG. 4. Partial rate (zeroth moment) as a function of the low cut q_{cut}^2 in the lepton pair invariant mass squared. The blue dashed line includes NLO corrections up to $1/m_b^2$, the black dotted line includes also $1/m_b^3$ corrections at LO, and the continuous red line includes NLO corrections up to $1/m_b^3$.



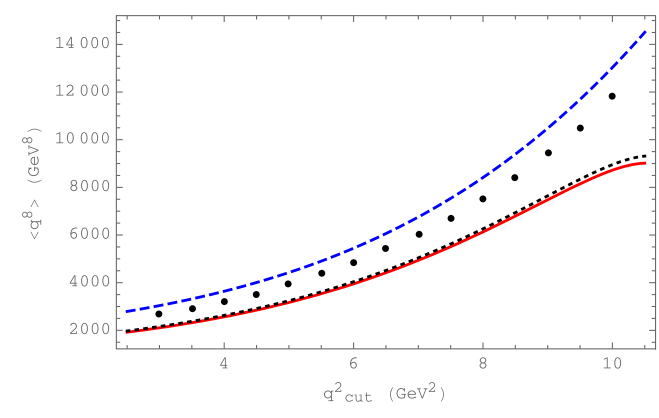
(a) First moment.



(b) Second moment.



(c) Third moment.



(d) Fourth moment.

FIG. 5. q^2 moments normalized to the partial rate as a function of the low cut q_{cut}^2 in the lepton pair invariant mass squared in the range $2.5 \text{ GeV}^2 < q_{\text{cut}}^2 < 10.5 \text{ GeV}^2$. The blue dashed line includes NLO corrections up to $1/m_b^2$, the black dotted line includes also $1/m_b^3$ corrections at LO, and the continuous red line includes NLO corrections up to $1/m_b^3$. Black dots correspond to experimental central values.

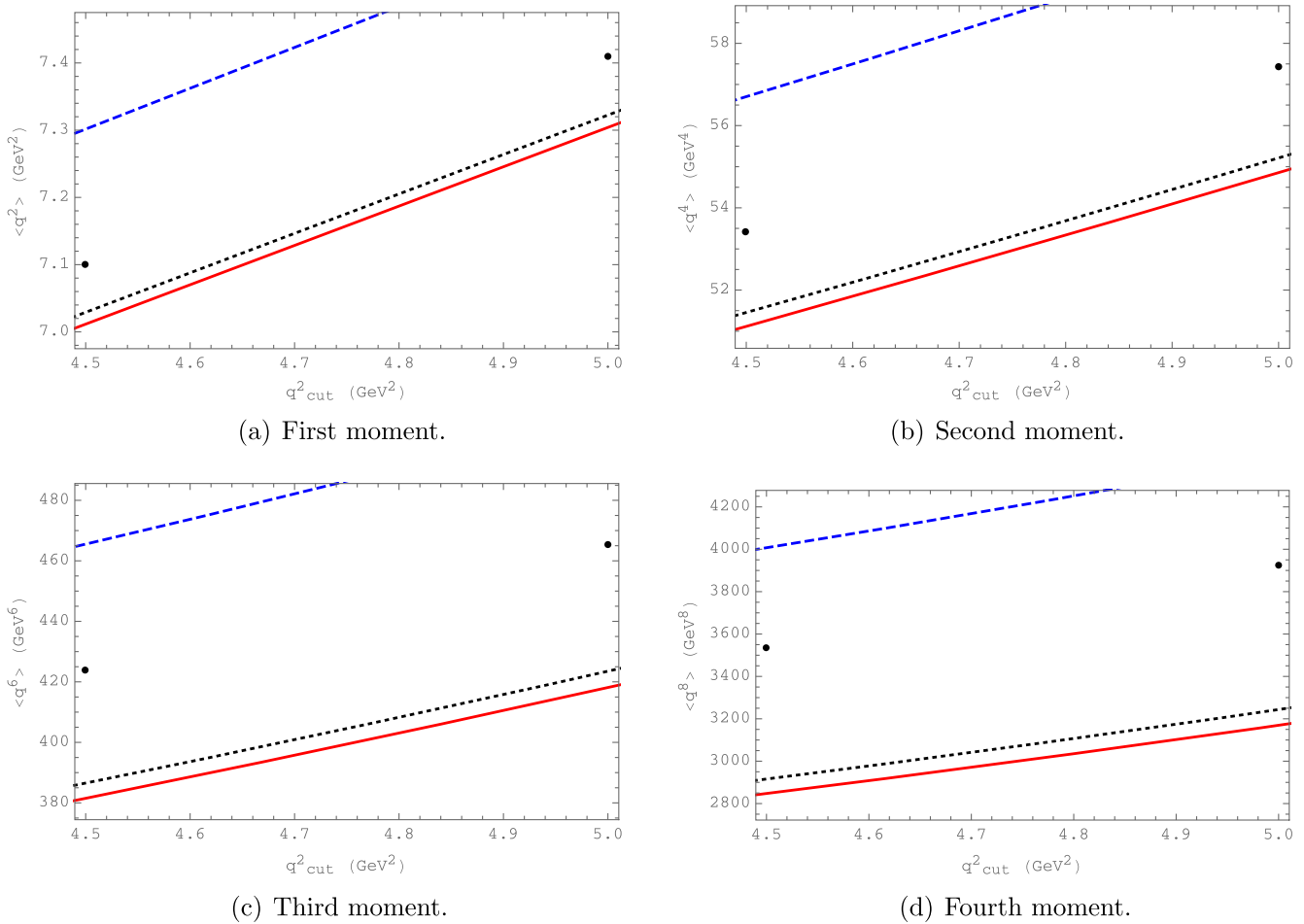


FIG. 6. q^2 moments normalized to the partial rate as a function of q_{cut}^2 in the range $4.5 \text{ GeV} < q_{\text{cut}}^2 < 5 \text{ GeV}$. The blue dashed line includes NLO corrections up to $1/m_b^2$, the black dotted line includes also $1/m_b^3$ corrections at LO, and the continuous red line includes NLO corrections up to $1/m_b^3$. Black dots correspond to experimental central values.

TABLE II. Numerical values for the coefficients of moments at different q_{cut}^2 .

	q_{cut}^2 (GeV^2)	$M_{n,0}^{\text{LO}}$	$M_{n,0}^{\text{NLO}}$	M_{n,μ_G}^{LO}	M_{n,μ_G}^{NLO}	M_{n,ρ_D}^{LO}	$M_{n,\rho_D}^{\text{NLO}}$
$M_0(q_{\text{cut}}^2)$	3.0	0.3835	-0.6332	-2.441	2.18	17.49	14.8
	4.5	0.2901	-0.4635	-2.439	2.07	16.89	15.4
	6.0	0.2056	-0.3146	-2.373	1.88	16.19	15.8
$M_1(q_{\text{cut}}^2)$	3.0	0.10938	-0.1736	-1.114	0.823	8.751	8.11
	4.5	0.09422	-0.1461	-1.113	0.804	8.651	8.21
	6.0	0.07501	-0.1123	-1.098	0.761	8.492	8.30
$M_2(q_{\text{cut}}^2)$	3.0	0.03527	-0.05371	-0.5230	0.329	4.584	4.37
	4.5	0.03278	-0.04919	-0.5228	0.326	4.568	4.39
	6.0	0.02838	-0.04146	-0.5192	0.316	4.531	4.41
$M_3(q_{\text{cut}}^2)$	3.0	0.01255	-0.01838	-0.2509	0.137	2.454	2.35
	4.5	0.01214	-0.01762	-0.2509	0.137	2.451	2.35
	6.0	0.01112	-0.01585	-0.2500	0.134	2.442	2.36
$M_4(q_{\text{cut}}^2)$	3.0	0.004809	-0.006795	-0.1223	0.0588	1.327	1.26
	4.5	0.004739	-0.006669	-0.1223	0.0587	1.326	1.26
	6.0	0.004504	-0.006257	-0.1221	0.0581	1.324	1.27

TABLE III. Numerical values for normalized moments $\langle q^{2n} \rangle = m_b^{2n} M_n / M_0$ at different q_{cut}^2 .

q_{cut}^2 (GeV 2)	$\langle q^2 \rangle$ (GeV 2)	$\langle q^4 \rangle$ (GeV 4)	$\langle q^6 \rangle$ (GeV 6)	$\langle q^8 \rangle$ (GeV 8)
3.0	6.134	41.13	291.8	2107
4.5	7.011	51.12	381.5	2847
6.0	7.887	62.90	502.3	3951

To discuss the impact of our result, we show the contribution to the partial rate, including a lower cut in q^2 , and its contribution to the first few (normalized) q^2 moments. Figures 4–6 show the dependence of these quantities on the lower cutoff q_{cut}^2 . In Figs. 4(b) and 6 we show the partial rate and normalized moments in a cut out range to perceive the difference between LO and NLO $1/m_b^3$ corrections. The NLO $1/m_b^3$ corrections represent around 1% of the total contribution to the normalized moments. Again, we use for illustration the numerical values given in Table I.

Some specific values for the coefficients of the (not yet normalized) moments at different q_{cut}^2 are given in Table II. We observe that the NLO $1/m_b^3$ corrections represent around a 5% correction of the LO $1/m_b^3$ correction. We also see that for larger moments there is less sensitivity to q_{cut}^2 .

Some specific values for the normalized moments are given in Table III.

VII. CONCLUSIONS

In the present paper, we have computed the NLO corrections up to order $1/m_b^3$ for the differential rate in the lepton pair invariant mass squared. Thus, the current knowledge of the HQE for the $B \rightarrow X_c \ell \bar{\nu}$ decay includes the NNLO corrections to the leading term for decay

distributions and the N³LO contributions to the total rate, together with the NLO corrections for decay distributions to order $1/m_b^2$ and $1/m_b^3$, while the terms at order $1/m_b^4$ and $1/m_b^5$ are known only at tree level.

The techniques developed in [44] can be extended to even higher orders, so the computation of the NLO contributions to the terms of order $1/m_b^4$ is technically possible. However, parametrically the largest unknown contributions are the NNLO corrections to the terms at order $1/m_b^2$, which are partially known for reparametrization invariant quantities due to the relation between the leading term and the coefficient of μ_π^2 .

Although the corrections we have computed here are not untypically large, they will have a visible impact on the determination of $|V_{cb}|$. This is mainly due to the fact that the coefficient in front of ρ_D in the total rate is quite large. While a detailed analysis will require to repeat the combined fit as, e.g., in Ref. [61], we may obtain a tendency from an approximate formula given in Eq. (12) in this paper.

ACKNOWLEDGMENTS

This research was supported by the Deutsche Forschungsgemeinschaft (DFG, German Research Foundation) under Grant No. 396021762-TRR 257 “Particle Physics Phenomenology after the Higgs Discovery.”

APPENDIX A: COEFFICIENTS OF THE DIFFERENTIAL DECAY WIDTH

In this Appendix we present the coefficients of the q^2 spectrum relevant for phenomenology. We also provide these expressions in the Supplemental Material [37] in *Mathematica* format.

Following Ref. [44], we define

$$x_- = \frac{1}{2} \left(1 - r + \rho - \sqrt{(1 - (\sqrt{r} - \sqrt{\rho})^2)(1 - (\sqrt{r} + \sqrt{\rho})^2)} \right), \quad (\text{A1})$$

$$x_+ = \frac{1}{2} \left(1 - r + \rho + \sqrt{(1 - (\sqrt{r} - \sqrt{\rho})^2)(1 - (\sqrt{r} + \sqrt{\rho})^2)} \right), \quad (\text{A2})$$

with $\rho = m_c^2/m_b^2$ and $r = q^2/m_b^2$. Furthermore, it is convenient to express some of the functions in terms of $L(x)$, which is the Roger’s dilogarithm

$$L(x) = \text{Li}_2(x) + \frac{1}{2} \ln(x) \ln(1-x) = \frac{1}{2} \left(\frac{\pi^2}{6} + \text{Li}_2(x) - \text{Li}_2(1-x) \right), \quad 0 < x < 1. \quad (\text{A3})$$

We define the full coefficients by

$$\mathcal{C}_i = \mathcal{C}_i^{\text{LO}} + \frac{\alpha_s}{\pi} (C_F \mathcal{C}_i^{\text{NLO,F}} + C_A \mathcal{C}_i^{\text{NLO,A}}), \quad (\text{A4})$$

with $i = 0, v, \mu_G, \rho_D$ and list below the coefficients of the right-hand side. The LO coefficients read

$$\mathcal{C}_0^{\text{LO}} = 48\pi^2(x_+ - x_-)(x_- x_+ (3x_- + 3x_+ - 8) + x_-(3 - 2x_-) + x_+(3 - 2x_+)), \quad (\text{A5})$$

$$\begin{aligned} \bar{\mathcal{C}}_v^{\text{LO}} = & -\frac{144\pi^2}{x_- - x_+} (x_-^2(2x_-^2 - 5x_- + 4) + x_+^2(2x_+^2 - 5x_+ + 4) - x_-^2x_+^2(x_- + x_+ - 4) \\ & - x_-x_+(3x_-^3 - 8x_-^2 + 7x_- + 3x_+^3 - 8x_+^2 + 7x_+)), \end{aligned} \quad (\text{A6})$$

$$\begin{aligned} \mathcal{C}_{\mu_G}^{\text{LO}} = & \frac{48\pi^2}{x_- - x_+} (x_-(10x_-^3 - 15x_-^2 + 4) + x_+(10x_+^3 - 15x_+^2 + 4) + 3x_-^2x_+^2(x_- + x_+ - 4) \\ & - x_-x_+(15x_-^3 - 28x_-^2 + 9x_- + 15x_+^3 - 28x_+^2 + 9x_+)), \end{aligned} \quad (\text{A7})$$

$$\begin{aligned} \mathcal{C}_{\rho_D}^{\text{LO}} = & \frac{16\pi^2}{(x_- - x_+)^3} (x_-^2(-10x_-^4 + 63x_-^3 - 120x_-^2 + 104x_- - 48) + x_+^2(-10x_+^4 + 63x_+^3 - 120x_+^2 + 104x_+ - 48) \\ & - 22x_-^3x_+^3(3x_- + 3x_+ - 16) + x_-^2x_+^2(3x_-^3 + 154x_-^2 - 570x_- + 3x_+^3 + 154x_+^2 - 570x_+ + 720) \\ & + x_-x_+(15x_-^5 - 80x_-^4 + 27x_-^3 + 240x_-^2 - 344x_- + 15x_+^5 - 80x_+^4 + 27x_+^3 + 240x_+^2 - 344x_+ + 192)). \end{aligned} \quad (\text{A8})$$

The NLO coefficients read

$$\mathcal{C}_0^{\text{NLO,A}} = 0, \quad (\text{A9})$$

$$\begin{aligned} \mathcal{C}_0^{\text{NLO,F}} = & -24\pi^2 \left\{ \frac{1}{2}(x_- - x_+)(x_-x_+(8x_-x_+ + 3x_- + 3x_+ - 28) + 3x_-(1 - 2x_-) + 3x_+(1 - 2x_+) + 8) \right. \\ & + 4(x_-x_+(3x_- + 3x_+ - 8) + x_-(3 - 2x_-) + x_+(3 - 2x_+)) \\ & \times \left[(x_- + x_+) \left(2L\left(1 - \frac{x_-}{x_+}\right) + L(x_-) - L(x_+) \right) - 2(x_- - x_+) \ln(x_+ - x_-) \right] + x_-(x_-^2x_+^2(4x_+ - 14) \\ & + x_-x_+(-14x_+^2 + 34x_+ + 26x_- - 40) + x_-(15 - 12x_-) + x_+(5x_+^2 - 4x_+ + 6)) \ln(x_-) - x_+(x_-^2x_+^2(4x_- - 14) \\ & + x_-x_+(-14x_-^2 + 34x_- + 26x_+ - 40) + x_+(15 - 12x_+) + x_-(5x_-^2 - 4x_- + 6)) \ln(x_+) - (4x_-^3x_+^3 - x_-^2x_+^2(14x_- \\ & + 14x_+ - 28) + x_-x_+(14x_+^2 - 12x_+ + 2x_-^2 + 12x_- - 28) + x_-(4x_-^2 - 14x_- + 14) + x_+(-4x_+^2 - 2x_+ + 14) - 4) \\ & \times \ln(1 - x_-) + (4x_-^3x_+^3 - x_-^2x_+^2(14x_- + 14x_+ - 28) + x_-x_+(14x_-^2 - 12x_- + 2x_+^2 + 12x_+ - 28) \\ & \left. + x_+(4x_+^2 - 14x_+ + 14) + x_-(4x_-^2 - 2x_- + 14) - 4) \ln(1 - x_+) \right\}, \end{aligned} \quad (\text{A10})$$

$$\bar{\mathcal{C}}_v^{\text{NLO,A}} = 0, \quad (\text{A11})$$

$$\begin{aligned} \bar{\mathcal{C}}_v^{\text{NLO,F}} = & -24\pi^2 \left\{ -4(18x_-^2x_+^2 + x_-x_+(9x_-^2 - 32x_- + 9x_+^2 - 32x_+ + 28) - 6x_-(x_- - 1)^2 \right. \\ & - 6x_+(x_+ - 1)^2) \left(2L\left(1 - \frac{x_-}{x_+}\right) + L(x_-) - L(x_+) \right) + 4(x_- - x_+)(5x_- + 5x_+ - 6)(3x_-x_+ - 2x_- - 2x_+ + 1) \ln(x_+ - x_-) \\ & + \frac{1}{2(x_- - x_+)} (48x_-^3x_+^3 + x_-^2x_+^2(-24x_-^2 + 87x_- - 24x_+^2 + 87x_+ - 352) + 2x_-^2(3x_-^2 + 5x_- - 17) \\ & + x_-x_+(9x_-^3 - 118x_-^2 + 278x_- + 9x_+^3 - 118x_+^2 + 278x_+ - 124) + 2x_+^2(3x_+^2 + 5x_+ - 17)) + (x_- - 1)(6x_-^2x_+^2(2x_+ - 7) \\ & + x_-x_+(12x_- - 30x_+^2 + 59x_+ - 4) + x_-(8x_- - 13) + x_+(12x_+^2 - 13x_+ - 6) + 5) \ln(1 - x_-) \\ & - (x_+ - 1)(6x_-^2x_+^2(2x_- - 7) + x_-x_+(12x_+ - 30x_-^2 + 59x_- - 4) + x_+(8x_+ - 13) + x_-(12x_-^2 - 13x_- - 6) + 5) \ln(1 - x_+) \\ & - \frac{x_-}{(x_- - x_+)^2} (x_-^2(-32x_-^2 + 29x_- + 12) + 3x_+^2(5x_+^3 - 2x_+^2 - 14x_+ + 8) + x_-^3x_+^3(12x_- - 24x_+ + 42) \\ & + x_-^2x_+^2(-43x_- - 42x_-^2 - 175x_+ + 42x_+^2 + 12x_+^3 + 266) + x_-x_+(-136x_- - 34x_-^2 + 72x_-^3 - 139x_+ + 94x_+^2 \\ & + 35x_+^3 - 42x_+^4 + 60)) \ln(x_-) + \frac{x_+}{(x_- - x_+)^2} (x_+^2(-32x_+^2 + 29x_+ + 12) + 3x_+^2(5x_-^3 - 2x_-^2 - 14x_- + 8) \\ & + x_-^3x_+^3(12x_+ - 24x_- + 42) + x_-^2x_+^2(-43x_+ - 42x_+^2 - 175x_- + 42x_-^2 + 12x_-^3 + 266) \\ & \left. + x_-x_+(-136x_+ - 34x_+^2 + 72x_+^3 - 139x_- + 94x_-^2 + 35x_-^3 - 42x_-^4 + 60)) \ln(x_+) \right\}, \end{aligned} \quad (\text{A12})$$

$$\begin{aligned} \mathcal{C}_{\mu_G}^{\text{NLO,A}} = & -16\pi^2 \left\{ -\frac{1}{4(x_- - x_+)} (9x_-^2 x_+^2 (x_- + x_+ + 12) + x_- x_+ (135x_-^3 - 348x_-^2 + 105x_- + 135x_+^3 - 348x_+^2 + 105x_+ + 40) \right. \\ & - x_- (90x_-^3 - 183x_-^2 + 20x_- + 48) - x_+ (90x_+^3 - 183x_+^2 + 20x_+ + 48)) \\ & - 2(9x_-^2 x_+^2 - 2x_- x_+ (7x_- + 7x_+ - 8) + 2x_- (4x_- - 3) + 2x_+ (4x_+ - 3) - 1) \times \left(2L \left(1 - \frac{x_-}{x_+} \right) + L(x_-) - L(x_+) \right) \\ & + \frac{x_- - x_+}{x_- x_+} (x_-^2 x_+^2 (9x_- + 9x_+ - 20) - 2x_- x_+ (3x_-^2 - x_- + 3x_+^2 - x_+ - 6) + x_- (6x_- - 7) + x_+ (6x_+ - 7)) \ln(x_+ - x_-) \\ & - \frac{x_- - 1}{2x_-} (17x_-^2 x_+^2 + x_- x_+ (9x_-^2 - 39x_- - 17x_+ + 29) - x_- (6x_-^2 - 19x_- + 11) + x_+ (6x_+ - 7)) \ln(1 - x_-) \\ & + \frac{x_+ - 1}{2x_+} (17x_-^2 x_+^2 + x_- x_+ (9x_+^2 - 39x_+ - 17x_- + 29) - x_+ (6x_+^2 - 19x_+ + 11) + x_- (6x_- - 7)) \ln(1 - x_+) \\ & + \frac{x_-}{2x_+ (x_- - 1)(x_- - x_+)^2} (x_-^3 x_+^3 (62x_- + 47x_+ - 266) - x_-^2 x_+^2 (9x_-^3 + 17x_-^2 - 142x_- - 44x_+^3 + 173x_+^2 - 311x_+ + 96) \\ & + x_- x_+ (6x_-^4 - 9x_-^3 - 13x_-^2 + 6x_- - 78x_+^4 + 188x_+^3 - 81x_+^2 - 90x_+ + 16) - 2x_-^2 (6x_-^2 - 13x_- + 7) \\ & + 2x_+^2 (20x_+^3 - 43x_+^2 + 5x_+ + 23)) \ln(x_-) - \frac{x_+}{2x_- (x_+ - 1)(x_- - x_+)^2} (x_-^3 x_+^3 (62x_+ + 47x_- - 266) \\ & - x_-^2 x_+^2 (9x_+^3 + 17x_+^2 - 142x_+ - 44x_-^3 + 173x_-^2 - 311x_- + 96) \\ & + x_- x_+ (6x_+^4 - 9x_+^3 - 13x_+^2 + 6x_+ - 78x_-^4 + 188x_-^3 - 81x_-^2 - 90x_- + 16) \\ & \left. - 2x_+^2 (6x_+^2 - 13x_+ + 7) + 2x_-^2 (20x_-^3 - 43x_-^2 + 5x_- + 23)) \ln(x_+) \right\}, \end{aligned} \quad (\text{A13})$$

$$\begin{aligned} \mathcal{C}_{\mu_G}^{\text{NLO,F}} = & -16\pi^2 \left\{ \frac{1}{4} (x_- - x_+) (x_- x_+ (120x_- x_+ + 117x_- + 117x_+ - 332) + (85 - 138x_-) x_- + (85 - 138x_+) x_+ + 48) \right. \\ & + 2(66x_-^2 x_+^2 + x_- x_+ (45x_-^2 - 122x_- + 45x_+^2 - 122x_+ + 86) - x_- (30x_-^2 - 37x_- + 4) \\ & - x_+ (30x_+^2 - 37x_+ + 4) - 4) \left(2L \left(1 - \frac{x_-}{x_+} \right) + L(x_-) - L(x_+) \right) - \frac{8(x_- - x_+)}{x_- x_+} (x_-^2 x_+^2 (15x_- + 15x_+ - 32) \\ & - x_- x_+ (10x_-^2 - 11x_- + 10x_+^2 - 11x_+) - (x_- - 1)x_- - (x_+ - 1)x_+) \ln(x_+ - x_-) + \frac{x_+ - 1}{x_+} (4(x_- - 1)x_- \\ & + x_+ (10x_+^2 - 17x_+ + 8) + 30x_-^3 x_+^3 - x_-^2 x_+^2 (75x_- + 105x_+ - 133) + x_- x_+ (30x_-^2 - 13x_- + 45x_+^2 - 13x_+ - 33)) \ln(1 - x_+) \\ & - \frac{x_- - 1}{x_-} (4(x_+ - 1)x_+ + x_- (10x_-^2 - 17x_- + 8) + 30x_-^3 x_+^3 - x_-^2 x_+^2 (75x_+ + 105x_- - 133) \\ & + x_- x_+ (30x_+^2 - 13x_+ + 45x_-^2 - 13x_- - 33)) \ln(1 - x_-) + \frac{x_-}{2x_+ (x_+ - 1)(x_- - x_+)^2} (30x_-^4 x_+^4 (2x_- - 4x_+ + 5) \\ & - 16(x_- - 1)^2 x_-^2 - x_-^3 x_+^3 (210x_-^2 + 136x_- - 60x_+^3 - 330x_+^2 + 901x_+ - 1486) \\ & + x_-^2 x_+^2 (330x_-^3 - 326x_-^2 - 464x_- - 270x_+^4 - 154x_+^3 + 1191x_+^2 - 1759x_+ + 452) \\ & - x_- x_+ (140x_-^4 - 217x_-^3 + x_-^2 + 84x_- - 285x_+^5 + 24x_+^4 + 638x_+^3 - 531x_+^2 - 228x_+ + 4) \\ & - x_+^2 (75x_+^4 + 44x_+^3 - 186x_+^2 - 16x_+ + 172)) \ln(x_-) - \frac{x_+}{2x_- (x_- - 1)(x_- - x_+)^2} (30x_-^4 x_+^4 (2x_+ - 4x_- + 5) \\ & - 16(x_+ - 1)^2 x_+^2 - x_+^3 x_-^3 (210x_+^2 + 136x_+ - 60x_-^3 - 330x_-^2 + 901x_- - 1486) \\ & + x_-^2 x_+^2 (330x_-^3 - 326x_-^2 - 464x_- - 270x_+^4 - 154x_-^3 + 1191x_-^2 - 1759x_- + 452) \\ & - x_- x_+ (140x_+^4 - 217x_+^3 + x_+^2 + 84x_+ - 285x_-^5 + 24x_-^4 + 638x_-^3 - 531x_-^2 - 228x_- + 4) \\ & \left. - x_-^2 (75x_-^4 + 44x_-^3 - 186x_-^2 - 16x_- + 172)) \ln(x_+) \right\}, \end{aligned} \quad (\text{A14})$$

$$\begin{aligned}
C_{\rho_D}^{\text{NLO,A}} = & -16\pi^2 \left\{ \frac{1}{9(x_- - 1)x_-(x_- - x_+)^3(x_+ - 1)x_+} (-2x_-^5 x_+^5 (555x_- + 555x_+ - 3794) + 51x_+^4 (2x_-^3 - 9x_+^2 + 13x_+ - 6) \right. \\
& + 2x_-^4 x_+^4 (150x_-^3 + 1493x_-^2 - 8881x_- + 150x_-^3 + 1493x_-^2 - 8881x_- + 18512) \\
& + x_-^3 x_+^3 (222x_-^5 - 1862x_-^4 + 103x_-^3 + 14137x_-^2 - 32312x_- + 222x_-^5 - 1862x_-^4 + 103x_-^3 + 14137x_-^2 - 32312x_- \\
& + 28792) + x_-^2 x_+^2 (-370x_-^6 + 2571x_-^5 - 4484x_-^4 + 62x_-^3 + 8379x_-^2 - 8942x_- + 370x_-^6 + 2571x_-^5 - 4484x_-^4 \\
& + 62x_-^3 + 8379x_-^2 - 8942x_- + 2748) + x_- x_+ (148x_-^7 - 1105x_-^6 + 2928x_-^5 - 3488x_-^4 + 1571x_-^3 - 48x_-^2 \\
& + 148x_-^7 - 1105x_-^6 + 2928x_-^5 - 3488x_-^4 + 1571x_-^3 - 48x_-^2) + 51x_-^4 (2x_-^3 - 9x_-^2 + 13x_- - 6)) \\
& + \frac{2}{3x_-^2(x_- - x_+)^3 x_+^2} (17(2x_- - 3)x_-^6 - 2x_+^5 x_-^5 (33x_- + 33x_+ - 206) - 4x_+^4 x_-^4 (6x_-^3 - 43x_-^2 + 162x_- + 6x_+^3 \\
& - 43x_-^2 + 162x_+ - 159) + x_+^3 x_-^3 (42x_-^5 - 110x_-^4 + 90x_-^3 + 279x_-^2 - 208x_- + 42x_-^5 - 110x_-^4 + 90x_-^3 + 279x_-^2 \\
& - 208x_+ + 168) - x_+^2 x_-^2 (28x_-^6 - 78x_-^5 + 78x_-^4 + 88x_-^3 + 93x_-^2 + 28x_-^6 - 78x_-^5 + 78x_-^4 + 88x_-^3 + 93x_-^2) \\
& + x_+ x_- (-39x_-^6 + 22x_-^5 + 108x_-^4 - 39x_-^3 + 22x_-^5 + 108x_-^4) + 17x_+^6 (2x_+ - 3)) \ln(x_+ - x_-) \\
& - \frac{2}{(x_- - x_+)^3} (x_-^3 x_+^3 (-9x_- - 9x_+ + 68) - 2x_-^2 x_+^2 (21x_-^3 - 77x_-^2 + 138x_- + 21x_+^3 - 77x_+^2 \\
& + 138x_+ - 180) + x_+^2 (-18x_-^4 + 51x_-^3 - 60x_-^2 + 47x_+ - 24) + x_- x_+ (27x_-^5 - 50x_-^4 - 15x_-^3 + 120x_-^2 - 167x_- \\
& + 27x_+^5 - 50x_+^4 - 15x_+^3 + 120x_+^2 - 167x_+ + 96) + x_-^2 (-18x_-^4 + 51x_-^3 - 60x_-^2 + 47x_- - 24)) \ln\left(\frac{\mu}{m_b}\right) \\
& + 2(15x_-^2 x_+^2 - 6x_- x_+ (3x_- + 3x_+ - 5) + 2x_+ (4x_+ - 9) + 2x_- (4x_- - 9) + 11) \left(2L\left(1 - \frac{x_-}{x_+}\right) + L(x_-) - L(x_+) \right) \\
& + \frac{1}{3(x_- - x_+)^3} \left[-\frac{(x_- - 1)}{x_-^2} (-63x_+^4 x_-^4 + x_-^4 (-28x_-^3 + 56x_-^2 - 46x_- + 15) + x_+^3 x_-^3 (-3x_-^2 + 203x_- + 33x_+^2 - 85x_+ - 31) \right. \\
& + x_+^2 x_-^2 (-57x_-^4 + 137x_-^3 - 277x_-^2 + 41x_- + 11x_+^3 + 5x_+^2 + 41x_+ + 78) + x_+ x_- (42x_-^6 - 46x_-^5 - 46x_-^4 + 161x_-^3 - 84x_-^2 \\
& + 5x_-^4 + 29x_-^3 - 108x_-^2) + 17x_+^4 (3 - 2x_+)) \ln(1 - x_-) - \frac{(x_+ - 1)}{x_+^2} (-63x_+^4 x_-^4 + 17x_-^4 (3 - 2x_-) \\
& + x_+^3 x_-^3 (33x_-^2 - 85x_- - 3x_+^2 + 203x_+ - 31) + x_+^2 x_-^2 (-57x_+^4 + 137x_+^3 - 277x_+^2 + 41x_+ + 11x_-^3 + 5x_-^2 + 41x_- + 78) \\
& + x_+ x_- (5x_-^4 + 29x_-^3 - 108x_-^2 + 42x_-^6 - 46x_-^5 - 46x_-^4 + 161x_-^3 - 84x_-^2) \\
& \left. + x_+^4 (-28x_-^3 + 56x_-^2 - 46x_- + 15)) \ln(1 - x_+) \right] \\
& + \frac{1}{3(x_- - x_+)^4} \left[\frac{1}{x_-^2(x_+ - 1)^2} (-552x_-^6 x_+^6 + 34(x_+ - 1)^2 (2x_+ - 3)x_+^5 + 2x_-^5 x_+^5 (96x_-^2 + 839x_- + 75x_+^2 + 482x_+ - 2305) \right. \\
& - x_-^4 x_+^4 (3x_-^4 + 554x_-^3 + 2116x_-^2 - 7850x_- + 69x_-^4 - 25x_-^3 + 1204x_-^2 - 4766x_- + 7948) \\
& + x_-^3 x_+^3 (42x_-^6 - 122x_-^5 + 420x_-^4 - 474x_-^3 + 106x_-^2 + 374x_- + 5x_-^5 + 678x_-^4 + 1088x_-^3 - 6530x_-^2 + 7024x_- - 862) \\
& + x_-^2 x_+^2 (-22x_-^6 - 426x_-^5 + 283x_-^4 + 2116x_-^3 - 2870x_-^2 + 528x_- - 28x_-^7 + 86x_-^6 - 48x_-^5 - 315x_-^4 + 171x_-^3 + 540x_-^2 \\
& - 408x_+) + x_- x_+ (42x_-^7 + 68x_-^6 - 429x_-^5 + 154x_-^4 + 246x_-^3 + 318x_-^3 - 660x_-^4 + 288x_-^5 + 132x_-^6 - 78x_-^7) \\
& - 6x_-^5 (4x_-^3 - 9x_-^2 - 3x_- + 9)) \ln(x_+) - \frac{1}{(x_- - 1)^2 x_+^2} (-552x_-^6 x_+^6 + 2x_-^5 x_+^5 (75x_-^2 + 482x_- + 96x_+^2 + 839x_+ - 2305) \\
& - 6x_-^5 (4x_-^3 - 9x_-^2 - 3x_- + 9) - x_-^4 x_+^4 (69x_-^4 - 25x_-^3 + 1204x_-^2 - 4766x_- + 3x_-^4 + 554x_-^3 + 2116x_-^2 - 7850x_- + 7948) \\
& \left. + x_-^3 x_+^3 (42x_-^6 - 122x_-^5 + 420x_-^4 - 474x_-^3 + 106x_-^2 + 374x_- + 5x_-^5 + 678x_-^4 + 1088x_-^3 - 6530x_-^2 + 7024x_- - 862) \right]
\end{aligned}$$

$$\begin{aligned}
& + x_-^2 x_+^2 (-28x_-^7 + 86x_-^6 - 48x_-^5 - 315x_-^4 + 171x_-^3 + 540x_-^2 - 408x_- - 22x_+^6 - 426x_+^5 + 283x_+^4 + 2116x_+^3 - 2870x_+^2 \\
& + 528x_+) + x_- x_+ (-78x_-^7 + 132x_-^6 + 288x_-^5 - 660x_-^4 + 318x_-^3 + 42x_+^7 + 68x_+^6 - 429x_+^5 \\
& + 154x_+^4 + 246x_+^3) + 34(x_- - 1)^2 x_-^5 (2x_- - 3)) \ln(x_-) \Big] \Big\}, \tag{A15}
\end{aligned}$$

$$\begin{aligned}
\mathcal{C}_{\rho_D}^{\text{NLO,F}} = & -4\pi^2 \left\{ -\frac{1}{3(x_- - 1)x_-(x_- - x_+)^3(x_+ - 1)x_+} (720x_-^6 x_+^6 - 6x_-^5 x_+^5 (80x_-^2 + 201x_- + 80x_+^2 \right. \\
& + 201x_+ - 1358) - 112x_+^4 (2x_-^3 - 9x_-^2 + 13x_+ - 6) + x_-^4 x_+^4 (120x_-^4 + 537x_-^3 + 1823x_-^2 \\
& - 14878x_- + 120x_+^4 + 537x_+^3 + 1823x_+^2 - 14878x_+ + 25684) + x_-^3 x_+^3 (-99x_-^5 + 726x_-^4 \\
& - 7148x_-^3 + 22367x_-^2 - 27606x_- - 99x_+^5 + 726x_+^4 - 7148x_+^3 + 22367x_+^2 - 27606x_+ \\
& + 19984) - x_-^2 x_+^2 (95x_-^6 + 1088x_-^5 - 8406x_-^4 + 18391x_-^3 - 16272x_-^2 + 7888x_- + 95x_+^6 \\
& + 1088x_+^5 - 8406x_+^4 + 18391x_+^3 - 16272x_+^2 + 7888x_+ - 2688) + x_- x_+ (74x_-^7 + 545x_-^6 \\
& - 3699x_-^5 + 6136x_-^4 - 2944x_-^3 - 96x_-^2 + x_+^2 (74x_+^5 + 545x_+^4 - 3699x_+^3 + 6136x_+^2 \\
& - 2944x_+ - 96)) - 112x_-^4 (2x_-^3 - 9x_-^2 + 13x_- - 6)) \\
& - \frac{32}{3x_-^2 (x_- - x_+) x_+^2} (7(3 - 2x_-) x_-^4 + x_+^4 x_-^4 (27x_- + 27x_+ - 92) + 3x_+^3 x_-^3 (x_-^3 - 10x_-^2 \\
& + 22x_- + x_+^3 - 10x_+^2 + 22x_+ - 36) - 2x_+^2 x_-^2 (x_-^4 + 27x_-^3 - 66x_-^2 + 10x_- + x_+^4 + 27x_+^3 \\
& - 66x_+^2 + 10x_+ + 3) + 2x_+ x_- (27x_-^4 - 52x_-^3 + 12x_-^2 + 27x_+^4 - 52x_+^3 + 12x_+^2) \\
& + 7x_+^4 (3 - 2x_+)) \ln(x_+ - x_-) \\
& - \frac{2}{3(x_- - x_+)^3} (-202x_-^3 x_+^3 (3x_- + 3x_+ - 16) + x_-^2 x_+^2 (-627x_-^3 + 3814x_-^2 - 8670x_- \\
& - 627x_+^3 + 3814x_+^2 - 8670x_+ + 11520) + x_+^2 (-310x_-^4 + 1233x_-^3 - 1920x_-^2 + 1664x_+ \\
& - 768) + x_- x_+ (465x_-^5 - 1280x_-^4 - 243x_-^3 + 3840x_-^2 - 5504x_- + 465x_+^5 - 1280x_+^4 \\
& - 243x_+^3 + 3840x_+^2 - 5504x_+ + 3072) + x_-^2 (-310x_-^4 + 1233x_-^3 - 1920x_-^2 + 1664x_- - 768)) \ln\left(\frac{\mu}{m_b}\right) \\
& - 8(42x_-^2 x_+^2 + x_+(-10x_+^2 + 55x_+ - 108) + x_- x_+ (15x_-^2 - 94x_- + 15x_+^2 - 94x_+ \\
& + 186) + x_-(-10x_-^2 + 55x_- - 108) + 56) \left(2L\left(1 - \frac{x_-}{x_+}\right) + L(x_-) - L(x_+) \right) \\
& + \frac{4}{3(x_- - x_+)} \left[\frac{x_- - 1}{x_-^2} (-30x_-^4 x_+^4 + 3x_-^3 x_+^3 (10x_-^2 + 10x_- + 25x_+ - 77) \right. \\
& + 28(2x_+ - 3)x_+^2 + x_-^2 x_+^2 (-105x_-^3 + 264x_-^2 + 80x_- - 30x_+^2 + 269x_+ - 499) \\
& + x_- x_+ (117x_-^4 - 503x_-^3 + 340x_-^2 + 124x_- - 160x_+^2 + 332x_+ - 96) \\
& \left. + x_-^2 (-38x_-^3 + 175x_-^2 - 128x_- + 12) \right) \ln(1 - x_-) \\
& + \frac{x_+ - 1}{x_+^2} (-30x_-^4 x_+^4 + 3x_-^3 x_+^3 (10x_+^2 + 10x_+ + 25x_- - 77) + x_-^2 x_+^2 (-105x_+^3 + 264x_+^2 \\
& + 80x_+ - 30x_-^2 + 269x_- - 499) + x_+^2 (-38x_+^3 + 175x_+^2 - 128x_+ + 12) + x_- x_+ (117x_+^4 \\
& - 503x_+^3 + 340x_+^2 + 124x_+ - 160x_-^2 + 332x_- - 96) + 28x_-^2 (2x_- - 3) \right) \ln(1 - x_+) \Big]
\end{aligned}$$

$$\begin{aligned}
& + \frac{2}{3(x_- - x_+)^4} \left[\frac{1}{(x_- - 1)^2 x_+^2} (-360x_-^7 x_+^7 + 12x_-^6 x_+^6 (20x_-^2 - 5x_- + 20x_+^2 + 95x_+ - 612) \right. \\
& - 24x_+^5 (4x_+^3 - 9x_-^2 - 3x_+ + 9) + x_-^5 x_+^5 (-60x_-^4 - 510x_-^3 + 2889x_-^2 + 8952x_- - 60x_+^4 \\
& - 1110x_+^3 + 228x_+^2 + 25208x_+ - 57447) + x_-^4 x_+^4 (210x_-^5 + 114x_-^4 - 5874x_-^3 + 5428x_-^2 \\
& + 35080x_- + 330x_+^5 + 1782x_+^4 - 5552x_+^3 - 31173x_+^2 + 96064x_+ - 82750) \\
& + x_-^3 x_+^3 (-186x_-^6 + 656x_-^5 + 4072x_-^4 - 16328x_-^3 + 12738x_-^2 + 9520x_- - 555x_+^6 - 1138x_+^5 \\
& + 8874x_+^4 + 12618x_+^3 - 66224x_+^2 + 67048x_+ - 15056) + x_-^2 x_+^2 (44x_-^7 - 1189x_-^6 + 1674x_-^5 \\
& + 4711x_-^4 - 10760x_-^3 + 6400x_-^2 - 888x_- + 360x_+^7 + 86x_+^6 - 5400x_+^5 + 3103x_+^4 + 15544x_+^3 \\
& - 20360x_+^2 + 4632x_+) + x_- x_+ (864x_-^7 - 2720x_-^6 + 2224x_-^5 + 256x_-^4 - 624x_-^3 - 75x_+^8 \\
& + 228x_+^7 + 902x_+^6 - 2784x_+^5 + 1168x_+^4 + 984x_+^3) - 112(x_- - 1)^2 x_-^5 (2x_- - 3)) \ln(x_-) \\
& + \frac{1}{x_+^2 (x_+ - 1)^2} (360x_-^7 x_+^7 - 12x_-^6 x_+^6 (20x_-^2 + 95x_- + 20x_+^2 - 5x_+ - 612) \\
& + 112(x_+ - 1)^2 (2x_+ - 3)x_+^5 + x_-^5 x_+^5 (60x_-^4 + 1110x_-^3 - 228x_-^2 - 25208x_- + 60x_+^4 + 510x_+^3 \\
& - 2889x_+^2 - 8952x_+ + 57447) - x_-^4 x_+^4 (330x_-^5 + 1782x_-^4 - 5552x_-^3 - 31173x_-^2 + 96064x_- \\
& + 210x_+^5 + 114x_+^4 - 5874x_+^3 + 5428x_+^2 + 35080x_+ - 82750) + x_-^3 x_+^3 (555x_-^6 + 1138x_-^5 - 8874x_-^4 \\
& - 12618x_-^3 + 66224x_-^2 - 67048x_- + 186x_-^6 - 656x_-^5 - 4072x_-^4 + 16328x_-^3 - 12738x_-^2 - 9520x_- \\
& + 15056) - x_-^2 x_+^2 (360x_-^7 + 86x_-^6 - 5400x_-^5 + 3103x_-^4 + 15544x_-^3 - 20360x_-^2 + 4632x_- + 44x_+^7 \\
& - 1189x_-^6 + 1674x_-^5 + 4711x_-^4 - 10760x_-^3 + 6400x_-^2 - 888x_-) + x_- x_+ (75x_-^8 - 228x_-^7 - 902x_-^6 \\
& + 2784x_-^5 - 1168x_-^4 - 984x_-^3 - 864x_-^2 + 2720x_-^6 - 2224x_-^5 - 256x_-^4 + 624x_-^3) \\
& \left. + 24x_-^5 (4x_-^3 - 9x_-^2 - 3x_- + 9) \right] \ln(x_+) \Bigg\}, \tag{A16}
\end{aligned}$$

APPENDIX B: DARWIN COEFFICIENTS FOR THE MOMENTS WITH LOW CUT

Here we present analytical expressions for the Darwin coefficients of the moments $M_n(r_{\text{cut}})$ defined in Eqs. (39) and (40), which depend on the low cut r_{cut} in the lepton pair invariant mass squared. We define

$$t_0 = \frac{1}{2} \ln \left(\frac{x_+(r_{\text{cut}})}{x_-(r_{\text{cut}})} \right). \tag{B1}$$

At LO, they read

$$\begin{aligned}
M_{0,\rho_D}^{\text{LO}}(r_{\text{cut}}) &= -\frac{4}{3}(5\rho + 21)\rho^{3/2} \sinh(3t_0) + 8(3\rho^2 + 4)t_0 + \frac{10}{3}\rho^2 \sinh(4t_0) - \frac{4}{3}(33\rho^2 + 153\rho + 104)\sqrt{\rho} \sinh(t_0) \\
&+ 16(5\rho^2 + 10\rho + 1) \coth(t_0) - 16(\rho^2 + 10\rho + 5)\sqrt{\rho} \operatorname{csch}(t_0) + \frac{40}{3}(5\rho + 6)\rho \sinh(2t_0), \tag{B2}
\end{aligned}$$

$$\begin{aligned}
M_{1,\rho_D}^{\text{LO}}(r_{\text{cut}}) &= -\frac{8}{3}\rho^{5/2} \sinh(5t_0) + \frac{1}{3}(25\rho + 73)\rho^2 \sinh(4t_0) + \frac{8}{3}(37\rho^2 + 109\rho + 56)\rho \sinh(2t_0) \\
&- \frac{4}{9}(15\rho^2 + 188\rho + 183)\rho^{3/2} \sinh(3t_0) + \frac{4}{3}(27\rho^3 - 69\rho^2 + 8\rho + 24)t_0 \\
&- \frac{4}{3}(33\rho^3 + 322\rho^2 + 377\rho + 152)\sqrt{\rho} \sinh(t_0) + 16(7\rho^3 + 35\rho^2 + 21\rho + 1) \coth(t_0) \\
&- 16(\rho^3 + 21\rho^2 + 35\rho + 7)\sqrt{\rho} \operatorname{csch}(t_0), \tag{B3}
\end{aligned}$$

$$\begin{aligned}
M_{2,\rho_D}^{\text{LO}}(r_{\text{cut}}) = & -\frac{4}{15}(35\rho + 83)\rho^{5/2} \sinh(5t_0) + \frac{20}{9}\rho^3 \sinh(6t_0) + \frac{8}{3}(5\rho^2 + 37\rho + 32)\rho^2 \sinh(4t_0) \\
& + \frac{4}{3}(98\rho^3 + 547\rho^2 + 610\rho + 188)\rho \sinh(2t_0) - \frac{4}{9}(15\rho^3 + 376\rho^2 + 880\rho + 407)\rho^{3/2} \sinh(3t_0) \\
& + \frac{16}{3}(9\rho^4 - 56\rho^3 - 131\rho^2 + 4\rho + 6)t_0 - \frac{4}{3}(33\rho^4 + 557\rho^3 + 997\rho^2 + 769\rho + 200)\sqrt{\rho} \sinh(t_0) \\
& + 16(9\rho^4 + 84\rho^3 + 126\rho^2 + 36\rho + 1) \coth(t_0) - 16(\rho^4 + 36\rho^3 + 126\rho^2 + 84\rho + 9)\sqrt{\rho} \operatorname{csch}(t_0), \quad (\text{B4})
\end{aligned}$$

$$\begin{aligned}
M_{3,\rho_D}^{\text{LO}}(r_{\text{cut}}) = & -\frac{40}{21}\rho^{7/2} \sinh(7t_0) + \frac{2}{3}(15\rho + 31)\rho^3 \sinh(6t_0) - \frac{4}{15}(75\rho^2 + 424\rho + 339)\rho^{5/2} \sinh(5t_0) \\
& + \frac{1}{3}(55\rho^3 + 747\rho^2 + 1515\rho + 663)\rho^2 \sinh(4t_0) - \frac{4}{3}(5\rho^4 + 209\rho^3 + 882\rho^2 + 921\rho + 261)\rho^{3/2} \sinh(3t_0) \\
& + 4(15\rho^5 - 165\rho^4 - 925\rho^3 - 585\rho^2 + 8\rho + 8)t_0 \\
& + \frac{2}{3}\sqrt{\rho}(\sqrt{\rho}(244\rho^4 + 2223\rho^3 + 4191\rho^2 + 2772\rho + 576) \sinh(2t_0) \\
& - 2(33\rho^5 + 858\rho^4 + 2200\rho^3 + 1938\rho^2 + 1377\rho + 248) \sinh(t_0)) \\
& + 16(11\rho^5 + 165\rho^4 + 462\rho^3 + 330\rho^2 + 55\rho + 1) \coth(t_0) \\
& - 16(\rho^5 + 55\rho^4 + 330\rho^3 + 462\rho^2 + 165\rho + 11)\sqrt{\rho} \operatorname{csch}(t_0), \quad (\text{B5})
\end{aligned}$$

$$\begin{aligned}
M_{4,\rho_D}^{\text{LO}}(r_{\text{cut}}) = & -\frac{4}{21}(55\rho + 103)\rho^{7/2} \sinh(7t_0) + \frac{5}{3}\rho^4 \sinh(8t_0) + \frac{8}{9}(30\rho^2 + 143\rho + 108)\rho^3 \sinh(6t_0) \\
& - \frac{4}{15}(130\rho^3 + 1291\rho^2 + 2371\rho + 1002)\rho^{5/2} \sinh(5t_0) \\
& + \frac{2}{3}(35\rho^4 + 752\rho^3 + 2666\rho^2 + 2640\rho + 723)\rho^2 \sinh(4t_0) \\
& + \frac{8}{3}(73\rho^5 + 988\rho^4 + 2815\rho^3 + 2916\rho^2 + 1377\rho + 206)\rho \sinh(2t_0) \\
& - \frac{4}{9}(15\rho^5 + 941\rho^4 + 6243\rho^3 + 11115\rho^2 + 6981\rho + 1359)\rho^{3/2} \sinh(3t_0) \\
& + \frac{8}{3}(27\rho^6 - 456\rho^5 - 4495\rho^4 - 6840\rho^3 - 2157\rho^2 + 16\rho + 12)t_0 \\
& - \frac{4}{3}(33\rho^6 + 1225\rho^5 + 4291\rho^4 + 2779\rho^3 + 2577\rho^2 + 2249\rho + 296)\sqrt{\rho} \sinh(t_0) \\
& + 16(13\rho^6 + 286\rho^5 + 1287\rho^4 + 1716\rho^3 + 715\rho^2 + 78\rho + 1) \coth(t_0) \\
& - 16(\rho^6 + 78\rho^5 + 715\rho^4 + 1716\rho^3 + 1287\rho^2 + 286\rho + 13)\sqrt{\rho} \operatorname{csch}(t_0), \quad (\text{B6})
\end{aligned}$$

at NLO the expressions are very lengthy and are provided in the Supplemental Material [37].

APPENDIX C: DARWIN COEFFICIENTS FOR MOMENTS

The moments integrated over the whole phase space can be obtained from the results of the previous section in the special case $r_{\text{cut}} = 0$. The zeroth moment, or total width, reads

$$M_{0,\rho_D}^{\text{LO}}(0) = C_{\rho_D}^{\text{LO}} = \frac{1}{3}(5\rho^4 + 8\rho^3 - 24\rho^2 - 12(3\rho^2 + 4)\ln(\rho) + 88\rho - 77), \quad (\text{C1})$$

$$\begin{aligned}
M_{0,\rho_D}^{\text{NLO,F}}(0) = C_{\rho_D}^{\text{NLO,F}} = & \frac{64}{9}(\rho^4 - 2\rho^3 - 3\rho^2 + 14\rho - 6\ln(\rho) - 10)\ln\left(\frac{\mu}{m_b}\right) + \frac{64}{9}\sqrt{\rho}(27\rho^2 + 16\rho + 13)\text{Li}_2(1 - \sqrt{\rho}) \\
& + \frac{1}{9}(-432\rho^{5/2} - 256\rho^{3/2} + 45\rho^4 + 24\rho^3 - 744\rho^2 + 768\rho - 208\sqrt{\rho} - 147)\text{Li}_2(1 - \rho) \\
& + \frac{1}{18}\rho(15\rho^3 - 16\rho^2 - 500\rho - 96)\ln^2(\rho) + \frac{1}{270}(255\rho^4 - 8\rho^3 - 23390\rho^2 + 780\rho - 6600)\ln(\rho) \\
& + \frac{1}{9}(15\rho^4 + 20\rho^3 + 256\rho^2 + 468\rho + 83)\ln(1 - \rho)\ln(\rho) + \frac{4305\rho^4 + 56740\rho^3 + 44072\rho^2 - 61044\rho - 41721}{1080} \\
& - \frac{(255\rho^5 + 3232\rho^4 + 9580\rho^3 - 5640\rho^2 - 5815\rho - 2200)\ln(1 - \rho)}{270\rho} - \frac{98}{45}\left(\frac{1}{\rho} + \frac{\ln(1 - \rho)}{\rho^2}\right), \tag{C2}
\end{aligned}$$

$$\begin{aligned}
M_{0,\rho_D}^{\text{NLO,A}}(0) = C_{\rho_D}^{\text{NLO,A}} = & \frac{2}{3}(9\rho^4 - 28\rho^3 + 18\rho^2 + 36\rho - 24\ln(\rho) - 35)\ln\left(\frac{\mu}{m_b}\right) + \frac{8}{9}\sqrt{\rho}(57\rho^2 + 50\rho - 35)\text{Li}_2(1 - \sqrt{\rho}) \\
& - \frac{2}{9}(57\rho^{5/2} + 50\rho^{3/2} + 69\rho^3 + 37\rho^2 + 108\rho - 35\sqrt{\rho} - 24)\text{Li}_2(1 - \rho) + \frac{1}{9}(-17\rho^3 - 23\rho^2 + 45\rho + 39)\ln^2(\rho) \\
& - \frac{2}{9}(26\rho^3 + 18\rho^2 + 75\rho - 1)\ln(1 - \rho)\ln(\rho) + \frac{1}{270}(420\rho^4 - 5117\rho^3 + 1455\rho^2 - 4290\rho + 6930)\ln(\rho) \\
& - \frac{1480\rho^4 - 5285\rho^3 + 701\rho^2 + 22203\rho - 19813}{540} - \frac{(420\rho^5 - 4097\rho^4 + 2295\rho^3 - 1740\rho^2 + 4160\rho - 1395)\ln(1 - \rho)}{270\rho} \\
& - \frac{119}{90}\left(\frac{1}{\rho} + \frac{\ln(1 - \rho)}{\rho^2}\right). \tag{C3}
\end{aligned}$$

Note that there is no $1/\rho$ singularity at small ρ . The same applies to higher moments. The first moment reads

$$M_{1,\rho_D}^{\text{LO}}(0) = \frac{1}{18}(-729 + 1831\rho - 1296\rho^2 + 144\rho^3 + 41\rho^4 + 9\rho^5 - 12(24 + 8\rho - 69\rho^2 + 27\rho^3)\ln(\rho)), \tag{C4}$$

$$\begin{aligned}
M_{1,\rho_D}^{\text{NLO,F}}(0) = & \frac{32}{135}(9\rho^5 - 25\rho^4 - 180\rho^3 - 540\rho^2 + 60(12\rho^2 - \rho - 3)\ln(\rho) + 1195\rho \\
& - 459)\ln\left(\frac{\mu}{m_b}\right) + \frac{64}{9}\sqrt{\rho}(27\rho^3 + 166\rho^2 - 145\rho + 40)\text{Li}_2(1 - \sqrt{\rho}) \\
& + \frac{1}{18}(-864\rho^{7/2} - 5312\rho^{5/2} + 4640\rho^{3/2} + 27\rho^5 + 103\rho^4 - 3952\rho^3 + 2832\rho^2 \\
& + 3303\rho - 1280\sqrt{\rho} - 485)\text{Li}_2(1 - \rho) + \frac{1}{36}\rho(9\rho^4 + 45\rho^3 - 2500\rho^2 + 92\rho \\
& - 640)\ln^2(\rho) + \frac{1}{540}(291\rho^5 + 1218\rho^4 - 142110\rho^3 - 19510\rho^2 - 12545\rho \\
& - 21120)\ln(\rho) + \frac{1}{18}(9\rho^5 + 29\rho^4 + 444\rho^3 + 2108\rho^2 + 1933\rho \\
& + 121)\ln(1 - \rho)\ln(\rho) + \frac{1}{3240\rho}(4077\rho^6 + 126439\rho^5 + 1536734\rho^4 \\
& - 1850526\rho^3 + 561605\rho^2 - 376649\rho - 1680) - \frac{1}{540\rho^2}(291\rho^7 + 4123\rho^6 \\
& + 23200\rho^5 + 62960\rho^4 - 75035\rho^3 - 14371\rho^2 - 1448\rho + 280)\ln(1 - \rho), \tag{C5}
\end{aligned}$$

$$\begin{aligned}
M_{1,\rho_D}^{\text{NLO,A}}(0) = & \frac{1}{45}(81\rho^5 - 425\rho^4 + 480\rho^3 - 3060\rho^2 + 60(33\rho^2 + \rho - 12)\ln(\rho) + 4655\rho - 1731)\ln\left(\frac{\mu}{m_b}\right) \\
& + \frac{8}{9}\sqrt{\rho}(57\rho^3 + 13\rho^2 + 435\rho - 89)\text{Li}_2(1 - \sqrt{\rho}) \\
& - \frac{1}{9}(114\rho^{7/2} + 26\rho^{5/2} + 870\rho^{3/2} + 97\rho^4 - 2\rho^3 + 1028\rho^2 + 526\rho - 178\sqrt{\rho} \\
& - 89)\text{Li}_2(1 - \rho) + \frac{1}{18}(-35\rho^4 + 44\rho^3 - 337\rho^2 + 174\rho + 78)\ln^2(\rho) \\
& - \frac{1}{9}(31\rho^4 + 70\rho^3 + 312\rho^2 + 326\rho - 11)\ln(1 - \rho)\ln(\rho) \\
& + \frac{1}{270}(126\rho^5 - 3719\rho^4 + 6350\rho^3 - 47625\rho^2 - 11260\rho + 8910)\ln(\rho) \\
& - \frac{666\rho^6 - 4767\rho^5 + 13987\rho^4 - 140085\rho^3 + 178068\rho^2 - 48124\rho + 255}{810\rho} \\
& - \frac{1}{270\rho^2}(126\rho^7 - 3089\rho^6 + 1630\rho^5 - 14925\rho^4 + 14470\rho^3 + 2249\rho^2 - 546\rho + 85)\ln(1 - \rho). \quad (\text{C6})
\end{aligned}$$

The second moment reads

$$M_{2,\rho_D}^{\text{LO}}(0) = \frac{2}{45}(-1119 + 4420\rho + 5275\rho^2 - 9200\rho^3 + 575\rho^4 + 44\rho^5 + 5\rho^6 - 60(6 + 4\rho - 131\rho^2 - 56\rho^3 + 9\rho^4)\ln(\rho)), \quad (\text{C7})$$

$$\begin{aligned}
M_{2,\rho_D}^{\text{NLO,F}}(0) = & \frac{32}{135}(4\rho^6 - 14\rho^5 - 275\rho^4 - 4600\rho^3 + 3200\rho^2 + 60(40\rho^3 + 70\rho^2 - 2\rho - 3)\ln(\rho) + 2246\rho - 561)\ln\left(\frac{\mu}{m_b}\right) \\
& + \frac{64}{9}\sqrt{\rho}(27\rho^4 + 424\rho^3 - 590\rho^2 - 600\rho + 67)\text{Li}_2(1 - \sqrt{\rho}) \\
& + \frac{2}{9}(-216\rho^{9/2} - 3392\rho^{7/2} + 4720\rho^{5/2} + 4800\rho^{3/2} + 3\rho^6 + 18\rho^5 - 1500\rho^4 \\
& - 752\rho^3 + 9989\rho^2 + 1394\rho - 536\sqrt{\rho} - 150)\text{Li}_2(1 - \rho) + \frac{1}{9}\rho(\rho^5 + 6\rho^4 - 908\rho^3 - 542\rho^2 + 2550\rho - 296)\ln^2(\rho) \\
& + \frac{1}{135}(44\rho^6 + 391\rho^5 - 65765\rho^4 - 62046\rho^3 + 121845\rho^2 - 7190\rho - 6522)\ln(\rho) \\
& + \frac{2}{9}(\rho^6 + 6\rho^5 + 100\rho^4 + 704\rho^3 + 1995\rho^2 + 798\rho + 22) \\
& \times \ln(1 - \rho)\ln(\rho) + \frac{1}{8100\rho}(4720\rho^7 + 235363\rho^6 + 9045850\rho^5 - 9532420\rho^4 \\
& - 2786860\rho^3 + 4462265\rho^2 - 1427358\rho - 1560) - \frac{1}{135\rho^2}(44\rho^8 + 858\rho^7 \\
& + 5055\rho^6 + 39924\rho^5 + 6450\rho^4 - 48794\rho^3 - 3383\rho^2 - 180\rho + 26)\ln(1 - \rho), \quad (\text{C8})
\end{aligned}$$

$$\begin{aligned}
M_{2,\rho_D}^{\text{NLO,A}}(0) = & \frac{2}{45}(18\rho^6 - 143\rho^5 + 250\rho^4 - 7900\rho^3 + 3950\rho^2 + 60(50\rho^3 + 130\rho^2 + \rho - 6)\ln(\rho) + 4907\rho - 1082)\ln\left(\frac{\mu}{m_b}\right) \\
& + \frac{8}{45}\sqrt{\rho}(285\rho^4 - 780\rho^3 + 10486\rho^2 + 6980\rho - 715)\text{Li}_2(1 - \sqrt{\rho}) \\
& - \frac{1}{45}(570\rho^{9/2} - 1560\rho^{7/2} + 20972\rho^{5/2} + 13960\rho^{3/2} + 339\rho^5 - 125\rho^4 + 8810\rho^3 + 34470\rho^2 + 4385\rho \\
& - 1430\sqrt{\rho} - 531)\text{Li}_2(1 - \rho) + \frac{1}{90}(-113\rho^5 + 295\rho^4 - 3160\rho^3 - 11180\rho^2 + 1410\rho + 390)\ln^2(\rho) \\
& - \frac{1}{45}(113\rho^5 + 465\rho^4 + 2790\rho^3 + 8850\rho^2 + 2695\rho - 77)\ln(1 - \rho)\ln(\rho) \\
& + \frac{1}{9450}(1960\rho^6 - 107302\rho^5 + 485730\rho^4 - 4731475\rho^3 - 9935345\rho^2 - 756140\rho + 355320)\ln(\rho) \\
& - \frac{1}{113400\rho}(41440\rho^7 - 699853\rho^6 + 10454561\rho^5 - 118412512\rho^4 + 60323932\rho^3 + 57175009\rho^2 \\
& - 8895837\rho + 13260) - \frac{1}{9450\rho^2}(1960\rho^8 - 90712\rho^7 + 30870\rho^6 - 1464855\rho^5 + 102375\rho^4 \\
& + 1384040\rho^3 + 45962\rho^2 - 10745\rho + 1105)\ln(1 - \rho).
\end{aligned} \tag{C9}$$

The third moment reads

$$\begin{aligned}
M_{3,\rho_D}^{\text{LO}}(0) = & \frac{1}{210}(-11897 + 66843\rho + 377475\rho^2 - 207025\rho^3 - 235375\rho^4 + 9597\rho^5 + 357\rho^6 + 25\rho^7) \\
& - 2(8 + 8\rho - 585\rho^2 - 925\rho^3 - 165\rho^4 + 15\rho^5)\ln(\rho),
\end{aligned} \tag{C10}$$

$$\begin{aligned}
M_{3,\rho_D}^{\text{NLO,F}}(0) = & \frac{32}{315}(5\rho^7 - 21\rho^6 - 861\rho^5 - 32375\rho^4 - 22925\rho^3 + 49245\rho^2 + 420(30\rho^4 + 125\rho^3 + 75\rho^2 - \rho - 1)\ln(\rho) \\
& + 8421\rho - 1489)\ln\left(\frac{\mu}{m_b}\right) + \frac{64}{315}\sqrt{\rho}(945\rho^5 + 27650\rho^4 - 44742\rho^3 - 206724\rho^2 - 52675\rho \\
& + 3290)\text{Li}_2(1 - \sqrt{\rho}) + \frac{1}{630}(-30240\rho^{11/2} - 884800\rho^{9/2} + 1431744\rho^{7/2} \\
& + 6615168\rho^{5/2} + 1685600\rho^{3/2} + 225\rho^7 + 2163\rho^6 - 282849\rho^5 - 732795\rho^4 \\
& + 5696425\rho^3 + 5460875\rho^2 + 294903\rho - 105280\sqrt{\rho} - 23379)\text{Li}_2(1 - \rho) \\
& + \frac{1}{1260}\rho(75\rho^6 + 721\rho^5 - 168623\rho^4 - 294105\rho^3 + 2277520\rho^2 + 1440740\rho - 63840)\ln^2(\rho) \\
& + \frac{1}{132300}(28125\rho^7 + 408534\rho^6 - 98525252\rho^5 - 237554415\rho^4 + 671252260\rho^3 + 615302485\rho^2 - 9618105\rho \\
& - 7279440)\ln(\rho) + \frac{1}{630}(75\rho^7 + 721\rho^6 + 12817\rho^5 + 89355\rho^4 + 641095\rho^3 + 791525\rho^2 + 165501\rho + 2287) \\
& \times \ln(1 - \rho)\ln(\rho) + \frac{1}{1587600\rho}(513975\rho^8 + 38403937\rho^7 + 3013994353\rho^6 - 1396552545\rho^5 \\
& - 12219126399\rho^4 + 9100014071\rho^3 + 1823764119\rho^2 - 360870391\rho - 141120) \\
& - \frac{1}{132300\rho^2}(28125\rho^9 + 747999\rho^8 + 3631243\rho^7 + 51208185\rho^6 + 143993115\rho^5 \\
& - 105515375\rho^4 - 90995499\rho^3 - 3003993\rho^2 - 105560\rho + 11760)\ln(1 - \rho),
\end{aligned} \tag{C11}$$

$$\begin{aligned}
M_{3,\rho_D}^{\text{NLO,A}}(0) = & \frac{1}{105}(45\rho^7 - 504\rho^6 + 1281\rho^5 - 96250\rho^4 - 115325\rho^3 + 178080\rho^2 + 420(70\rho^4 + 425\rho^3 + 300\rho^2 + \rho - 4) \\
& \times \ln(\rho) + 38479\rho - 5806) \ln\left(\frac{\mu}{m_b}\right) + \frac{8}{45}\sqrt{\rho}(285\rho^5 - 2285\rho^4 + 26034\rho^3 + 67734\rho^2 + 16225\rho - 985) \\
& \times \text{Li}_2(1 - \sqrt{\rho}) - \frac{1}{90}(1140\rho^{11/2} - 9140\rho^{9/2} + 104136\rho^{7/2} + 270936\rho^{5/2} + 64900\rho^{3/2} + 537\rho^6 - 718\rho^5 \\
& + 19905\rho^4 + 291560\rho^3 + 238785\rho^2 + 13002\rho - 3940\sqrt{\rho} - 1143)\text{Li}_2(1 - \rho) \\
& - \frac{1}{180}(179\rho^6 - 926\rho^5 + 6555\rho^4 + 115040\rho^3 + 81120\rho^2 - 4140\rho - 780)\ln^2(\rho) \\
& - \frac{1}{90}(179\rho^6 + 1134\rho^5 + 8655\rho^4 + 60560\rho^3 + 55575\rho^2 + 7974\rho - 181)\ln(1 - \rho)\ln(\rho) \\
& + \frac{1}{18900}(2100\rho^7 - 185481\rho^6 + 1615714\rho^5 - 18193665\rho^4 - 99214640\rho^3 - 68413730\rho^2 - 2551920\rho \\
& + 774060)\ln(\rho) - \frac{1}{226800\rho}(44400\rho^8 - 1291087\rho^7 + 43744586\rho^6 - 591368493\rho^5 - 675628320\rho^4 \\
& + 1038554743\rho^3 + 207381654\rho^2 - 21449723\rho + 12240) - \frac{1}{6300\rho^2}(700\rho^9 - 52867\rho^8 + 1158\rho^7 - 1969695\rho^6 \\
& - 3476340\rho^5 + 3752175\rho^4 + 1733242\rho^3 + 15967\rho^2 - 4680\rho + 340)\ln(1 - \rho). \tag{C12}
\end{aligned}$$

Finally, the fourth moment reads

$$\begin{aligned}
M_{4,\rho_D}^{\text{LO}}(0) = & \frac{1}{630}(-39213 + 295376\rho + 3814356\rho^2 + 1916880\rho^3 - 4547200\rho^4 - 1484112\rho^5 + 42924\rho^6 + 944\rho^7 + 45\rho^8 \\
& - 840(12 + 16\rho - 2157\rho^2 - 6840\rho^3 - 4495\rho^4 - 456\rho^5 + 27\rho^6)\ln(\rho)), \tag{C13}
\end{aligned}$$

$$\begin{aligned}
M_{4,\rho_D}^{\text{NLO,F}}(0) = & \frac{32}{945}(9\rho^8 - 44\rho^7 - 3234\rho^6 - 214620\rho^5 - 568400\rho^4 + 268716\rho^3 + 485394\rho^2 + 420(168\rho^5 + 1225\rho^4 \\
& + 1764\rho^3 + 546\rho^2 - 4\rho - 3)\ln(\rho) + 37084\rho - 4905) \ln\left(\frac{\mu}{m_b}\right) + \frac{64}{315}\sqrt{\rho}(945\rho^6 + 44240\rho^5 - 69919\rho^4 \\
& - 925752\rho^3 - 832349\rho^2 - 105560\rho + 4235)\text{Li}_2(1 - \sqrt{\rho}) + \frac{1}{630}(-30240\rho^{13/2} - 1415680\rho^{11/2} + 2237408\rho^{9/2} \\
& + 29624064\rho^{7/2} + 26635168\rho^{5/2} + 3377920\rho^{3/2} + 135\rho^8 + 1896\rho^7 - 355152\rho^6 - 1979544\rho^5 \\
& + 15640520\rho^4 + 37972200\rho^3 + 14596736\rho^2 + 417608\rho - 135520\sqrt{\rho} - 25089)\text{Li}_2(1 - \rho) \\
& + \frac{1}{1260}\rho(45\rho^7 + 632\rho^6 - 209944\rho^5 - 723128\rho^4 + 7807380\rho^3 + 14560000\rho^2 + 3845240\rho - 89600)\ln^2(\rho) \\
& + \frac{1}{793800}(116685\rho^8 + 2469368\rho^7 - 814929696\rho^6 - 3753287832\rho^5 + 12993499260\rho^4 + 31919295240\rho^3 \\
& + 11621886360\rho^2 - 61408200\rho - 47864880)\ln(\rho) + \frac{1}{630}(45\rho^8 + 632\rho^7 + 11816\rho^6 + 27832\rho^5 \\
& + 982940\rho^4 + 2898840\rho^3 + 1823192\rho^2 + 229176\rho + 1717)\ln(1 - \rho)\ln(\rho) \\
& + \frac{1}{19051200\rho}(3824955\rho^9 + 398946984\rho^8 + 53438905548\rho^7 + 31280266104\rho^6 \\
& - 690322598704\rho^5 + 34934038344\rho^4 + 537272304948\rho^3 + 38170138072\rho^2 \\
& - 5174932491\rho - 893760) - \frac{1}{793800\rho^2}(116685\rho^{10} + 4096448\rho^9 + 11921784\rho^8 \\
& + 194037648\rho^7 + 2485981680\rho^6 + 982489200\rho^5 - 2771006448\rho^4 \\
& - 891056784\rho^3 - 16195773\rho^2 - 421680\rho + 37240)\ln(1 - \rho), \tag{C14}
\end{aligned}$$

$$\begin{aligned}
M_{4,\rho_D}^{\text{NLO,A}}(0) = & \frac{1}{315} (81\rho^8 - 1216\rho^7 + 4284\rho^6 - 585480\rho^5 - 2172100\rho^4 + 706944\rho^3 + 1894116\rho^2 \\
& + 840(186\rho^5 + 1975\rho^4 + 3288\rho^3 + 1122\rho^2 + 2\rho - 6) \ln(\rho) + 172616\rho - 19245) \ln\left(\frac{\mu}{m_b}\right) \\
& + \frac{8}{315} \sqrt{\rho} (1995\rho^6 - 31150\rho^5 + 335545\rho^4 + 2063436\rho^3 \\
& + 1750189\rho^2 + 220290\rho - 8785) \text{Li}_2(1 - \sqrt{\rho}) \\
& - \frac{2}{315} (1995\rho^{13/2} - 31150\rho^{11/2} + 335545\rho^{9/2} + 2063436\rho^{7/2} + 1750189\rho^{5/2} \\
& + 220290\rho^{3/2} + 780\rho^7 - 2128\rho^6 + 19943\rho^5 + 1425935\rho^4 + 2874095\rho^3 \\
& + 1064175\rho^2 + 31787\rho - 8785\sqrt{\rho} - 2097) \text{Li}_2(1 - \rho) \\
& - \frac{1}{315} (260\rho^7 - 2226\rho^6 + 2086\rho^5 + 587440\rho^4 + 1163470\rho^3 + 375060\rho^2 \\
& - 9975\rho - 1365) \ln^2(\rho) - \frac{2}{315} (260\rho^7 + 2324\rho^6 + 21231\rho^5 + 278075\rho^4 \\
& + 529655\rho^3 + 230475\rho^2 + 19299\rho - 349) \ln(1 - \rho) \ln(\rho) \\
& + \frac{1}{396900} (26460\rho^8 - 3456445\rho^7 + 48877983\rho^6 - 590407188\rho^5 - 6662388180\rho^4 \\
& - 10471753530\rho^3 - 3776755290\rho^2 - 82403160\rho + 17302320) \ln(\rho) \\
& - \frac{1}{4762800\rho} (559440\rho^9 - 25054275\rho^8 + 1507458405\rho^7 - 22969818054\rho^6 \\
& - 93162469858\rho^5 + 29692805439\rho^4 + 78511998867\rho^3 + 6959893726\rho^2 \\
& - 515509350\rho + 135660) - \frac{1}{396900\rho^2} (26460\rho^{10} - 2980165\rho^9 - 1295217\rho^8 \\
& - 209585628\rho^7 - 1023663900\rho^6 + 147276360\rho^5 + 914828040\rho^4 \\
& + 175288092\rho^3 + 304128\rho^2 - 209475\rho + 11305) \ln(1 - \rho). \tag{C15}
\end{aligned}$$

The coefficients are also provided in the Supplemental Material [37].

-
- [1] M. A. Shifman and M. B. Voloshin, Sov. J. Nucl. Phys. **47**, 511 (1988).
- [2] E. Eichten and B. R. Hill, Phys. Lett. B **234**, 511 (1990).
- [3] N. Isgur and M. B. Wise, Phys. Lett. B **232**, 113 (1989).
- [4] B. Grinstein, Nucl. Phys. **B339**, 253 (1990).
- [5] J. Chay, H. Georgi, and B. Grinstein, Phys. Lett. B **247**, 399 (1990).
- [6] I. I. Y. Bigi, N. G. Uraltsev, and A. I. Vainshtein, Phys. Lett. B **293**, 430 (1992); **297**, 477(E) (1992).
- [7] B. Blok, L. Koyrakh, M. A. Shifman, and A. I. Vainshtein, Phys. Rev. D **49**, 3356 (1994); **50**, 3572(E) (1994).
- [8] A. V. Manohar and M. B. Wise, Phys. Rev. D **49**, 1310 (1994).
- [9] T. Mannel and K. K. Vos, J. High Energy Phys. 06 (2018) 115.
- [10] M. Fael, T. Mannel, and K. Keri Vos, J. High Energy Phys. 02 (2019) 177.
- [11] A. Czarnecki, M. Jezabek, and J. H. Kuhn, Acta Phys. Pol. B **20**, 961 (1989).
- [12] M. Gremm and I. W. Stewart, Phys. Rev. D **55**, 1226 (1997).
- [13] A. F. Falk and M. E. Luke, Phys. Rev. D **57**, 424 (1998).
- [14] A. F. Falk, M. E. Luke, and M. J. Savage, Phys. Rev. D **53**, 2491 (1996).
- [15] M. Trott, Phys. Rev. D **70**, 073003 (2004).
- [16] V. Aquila, P. Gambino, G. Ridolfi, and N. Uraltsev, Nucl. Phys. **B719**, 77 (2005).
- [17] A. Czarnecki and K. Melnikov, Phys. Rev. Lett. **78**, 3630 (1997).
- [18] A. Czarnecki and K. Melnikov, Phys. Rev. D **59**, 014036 (1998).
- [19] K. Melnikov, Phys. Lett. B **666**, 336 (2008).

- [20] A. Pak and A. Czarnecki, Phys. Rev. Lett. **100**, 241807 (2008).
- [21] A. Pak and A. Czarnecki, Phys. Rev. D **78**, 114015 (2008).
- [22] M. Dowling, A. Pak, and A. Czarnecki, Phys. Rev. D **78**, 074029 (2008).
- [23] S. Biswas and K. Melnikov, J. High Energy Phys. 02 (2010) 089.
- [24] P. Gambino, J. High Energy Phys. 09 (2011) 055.
- [25] M. Fael, K. Schönwald, and M. Steinhauser, Phys. Rev. D **104**, 016003 (2021).
- [26] T. Becher, H. Boos, and E. Lunghi, J. High Energy Phys. 12 (2007) 062.
- [27] A. Alberti, T. Ewerth, P. Gambino, and S. Nandi, Nucl. Phys. **B870**, 16 (2013).
- [28] A. Alberti, P. Gambino, and S. Nandi, J. High Energy Phys. 01 (2014) 147.
- [29] T. Mannel, A. A. Pivovarov, and D. Rosenthal, Phys. Lett. B **741**, 290 (2015).
- [30] T. Mannel, A. A. Pivovarov, and D. Rosenthal, Nucl. Part. Phys. Proc. **263–264**, 44 (2015).
- [31] T. Mannel, A. A. Pivovarov, and D. Rosenthal, Phys. Rev. D **92**, 054025 (2015).
- [32] M. Gremm and A. Kapustin, Phys. Rev. D **55**, 6924 (1997).
- [33] T. Mannel, A. V. Rusov, and F. Shahriaran, Nucl. Phys. **B921**, 211 (2017).
- [34] T. Mannel and A. A. Pivovarov, Phys. Rev. D **100**, 093001 (2019).
- [35] I. Bigi, T. Mannel, S. Turczyk, and N. Uraltsev, J. High Energy Phys. 04 (2010) 073.
- [36] T. Mannel, S. Turczyk, and N. Uraltsev, J. High Energy Phys. 11 (2010) 109.
- [37] See Supplemental Material at <http://link.aps.org/supplemental/10.1103/PhysRevD.105.054033> for analytical results in Mathematica format for the coefficients of the differential rate and moments of the distribution.
- [38] I. I. Y. Bigi, M. A. Shifman, N. G. Uraltsev, and A. I. Vainshtein, Phys. Rev. Lett. **71**, 496 (1993).
- [39] T. Mannel, W. Roberts, and Z. Ryzak, Nucl. Phys. **B368**, 204 (1992).
- [40] A. V. Manohar, Phys. Rev. D **56**, 230 (1997).
- [41] D. Benson, I. I. Bigi, T. Mannel, and N. Uraltsev, Nucl. Phys. **B665**, 367 (2003).
- [42] A. V. Manohar, Phys. Rev. D **82**, 014009 (2010).
- [43] T. van Ritbergen, Phys. Lett. B **454**, 353 (1999).
- [44] T. Mannel, D. Moreno, and A. A. Pivovarov, Phys. Rev. D **104**, 114035 (2021).
- [45] R. Lee, arXiv:1212.2685.
- [46] R. N. Lee, J. Phys. Conf. Ser. **523**, 012059 (2014).
- [47] M. Jamin and M. E. Lautenbacher, Comput. Phys. Commun. **74**, 265 (1993).
- [48] T. Huber and D. Maitre, Comput. Phys. Commun. **175**, 122 (2006).
- [49] T. Huber and D. Maitre, Comput. Phys. Commun. **178**, 755 (2008).
- [50] A. Grozin, arXiv:hep-ph/0508242.
- [51] A. F. Falk, B. Grinstein, and M. E. Luke, Nucl. Phys. **B357**, 185 (1991).
- [52] C. W. Bauer and A. V. Manohar, Phys. Rev. D **57**, 337 (1998).
- [53] M. Finkemeier and M. McIrvin, Phys. Rev. D **55**, 377 (1997).
- [54] C. Balzereit and T. Ohl, Phys. Lett. B **386**, 335 (1996).
- [55] B. Blok, J. G. Korner, D. Pirjol, and J. C. Rojas, Nucl. Phys. **B496**, 358 (1997).
- [56] C. L. Y. Lee, California Institute of Technology Report No. CALT-68-1663, 1991.
- [57] D. Moreno and A. Pineda, Phys. Rev. D **97**, 016012 (2018); **98**, 059902(E) (2018).
- [58] X. Lobregat, D. Moreno, and R. Petrossian-Byrne, Phys. Rev. D **97**, 054018 (2018).
- [59] D. Moreno, Phys. Rev. D **98**, 034016 (2018).
- [60] R. van Tonder *et al.* (Belle Collaboration), Phys. Rev. D **104**, 112011 (2021).
- [61] P. Gambino and C. Schwanda, Phys. Rev. D **89**, 014022 (2014).